DEVELOPMENT OF DESIGN PARAMETERS FOR SCALING UP A FLUIDIZED BED GASIFICATION SYSTEM

A Thesis

by

WALTER OOSTHUIZEN

Submitted to the Office of Graduate and Professional Studies of
Texas A&M University
in partial fulfillment of the requirements for the degree of

MASTER OF SCIENCE

Chair of Committee,	Calvin Parnell
Committee Members,	Sergio Capareda
	Dennis O'Neal
Head of Department,	Stephen Searcy

December 2015

Major Subject: Biological and Agricultural Engineering

ABSTRACT

Cotton gins across the globe accumulate cotton gin trash (CGT) as a byproduct from the ginning process. CGT is typically viewed as a waste product, however, it is a biomass that has an energy content of around 15.5 MJ kg^{-1}. The energy from the CGT can be converted to useful energy through fluidized bed gasification (FBG), which is a thermo-chemical process that converts a biomass into a combustible synthesis gas (syngas). The syngas can be combusted in an internal combustion engine to generate electricity.

Ambient air fluidization tests were conducted to validate a model to predict the minimum fluidization velocity (MFV) at hot, operating conditions of the gasifier. The average measured and the theoretical MFV at ambient conditions were found to be 56.0 and 63.5 cm s^{-1}, respectively. The percent error between the actual and theoretical MFV values at ambient conditions was 11.8%.

A tube cyclone was designed using the Texas A&M cyclone design (TCD) method and was implemented into the gasification system to partially separate the biochar from the syngas. The vortex inverter position within the cyclone and the flow rate of air were varied to determine the effect on capture efficiency. Capture efficiencies at ambient conditions ranged between 95% and 99%. The p-value of the tested flow rate and vortex inverter positions were 0.058 and 0.118, respectively, and had an insignificant effect on the capture efficiency of the cyclone. The estimated capture efficiency during gasification was deemed inconclusive and that additional research was needed to obtain an accurate efficiency.

The energy loading (EL) and fuel to air (F/A) ratio were the two operating parameters used when conducting gasification tests on a 0.15 m diameter gasifier. Lower heating values (LHV) of the syngas ranged between 5.25 and 2.76 MJ Nm^{-3} at F/A ratios of 0.6 and 0.96 kg_{fuel}/kg_{air}, respectively. At an optimum combination of EL of 17.0 GJ h^{-1} m^{-2} and a F/A ratio of 0.7 kg_{fuel}/kg_{air}, the average LHV of the syngas was approximately 4.72 MJ Nm^{-3} at an average reaction temperature of 700°C. The conversion of fuel to syngas by mass and energy were 39% and 38%, respectively.

The syngas produced from the FBG system was partially directed to a 4 kW generator during gasification. The engine of the generator was successfully fueled solely by syngas, which validated the concept that the pilot scale FBG system can be scaled up to generate 500 kW of electricity.

DEDICATION

To Dr. Parnell and Russell McGee, for their support, guidance, and assistance during this research. To my parents, Ingrid and Johan Oosthuizen. To my brothers, Jurgen, Johan, and Chris Oosthuizen. To my grandfather, Jurgen Schulz. To the Wolfram family, Stephanie, Ana Maria, and Pilar. To my goddaughter, Jocelynn.

ACKNOWLEDGEMENTS

I would like to acknowledge Dr. Parnell and Russell McGee for their endless support, encouragement, and suggestions throughout my graduate studies. All of our long discussions of ideas for this project motivated me to achieve success. I would also like to acknowledge my committee members, Dr. Dennis O'Neal and Dr. Sergio Capareda, for taking the time to help guide me for this research.

My parents, Ingrid and Johan Oosthuizen, along with my brothers, Jurgen, Johan, and Chris Oosthuizen, have been very supportive during my college career. Their encouragement always motivated me to keep my head up. My grandfather, Jurgen Schulz, has been the most influential person in my life. He shaped me to be the person I am today, and he will forever be my idol.

Last, but definitely not least, I would also like to thank Stephanie, Ana Maria, and Pilar Wolfram for their endless encouragement through my journey. You all always knew exactly how to show me the light when I needed it the most. You have all been family to me, always supporting me under any circumstance. For that, I will be forever grateful. My goddaughter, Jocelynn, is my biggest inspiration. The honor of having such a beautiful, intelligent, and kind-hearted girl in my life encourages me to strive for greatness.

NOMENCLATURE

$\Delta P_{cyclone}$	Pressure Drop through cyclone
Φ	Sphericity
ε_{mf}	Bed Voidage at Minimum Fluidization
$\eta_{cyclone}$	Capture Efficiency of Cyclone
η_e	Energy Conversion Efficiency
η_m	Conversion of Fuel to Gas by Mass
ρ_{gas}	Density of Gas
ρ_{ma}	Density of Moist Air
°C	Degrees Celsius
°F	Degrees Fahrenheit
µm	Micrometers
AC	Alternating Current
AED	Aerodynamic Equivalent Diameter
ANOVA	Analysis of Variance
Btu	British Thermal Unit
CGT	Cotton Gin Trash
D	Diameter of Cyclone
$\bar{d}_p$	Mean Particle Size
d_p*	Dimensionless Particle Size
EC	Energy Content
EC	Energy Content

EL	Energy Loading
ESD	Equivalent Spherical Diameter
F/A	Fuel to Air
FBG	Fluidized Bed Gasification
GSD	Geometric Standard Deviation
h	Hour
ICE	Internal Combustion Engine
kW	Kilowatt
LCV	Low Calorific Value
LFE	Laminar Flow Element
LHV	Lower Heating Value
MFV	Minimum Fluidization Velocity
min	Minute
MMD	Mass Median Diameter
MSW	Municipal Solid Waste
MW	Megawatt
Nm^3	Normal Cubic Meters
PSD	Particle Size Distribution
Q_{act}	Actual Volumetric Flow Rate
Q_{std}	Standard Volumetric Flow Rate
$Std.ft^3$	Standard Cubic Feet
TCD	Texas A&M Cyclone Design

V^*	Dimensionless Gas Velocity
V_{mf}	Minimum Fluidization Velocity
V_t	Terminal Velocity

TABLE OF CONTENTS

Page

LIST OF FIGURES

Page

LIST OF TABLES

Page

CHAPTER I

INTRODUCTION

In 2014, Texas ginned over 12 million bales of cotton (USDA, 2015). Seed cotton is typically harvested from the field mechanically with a stripper or a picker. The stripper can either be with or without a field cleaner. When the seed cotton is harvested from the field, a portion contains trash. The trash consists of burs, leaves, stalks, and soil. For a picker, stripper with a cleaner, and stripper without a cleaner, there is approximately 45, 180, and 360 kg of trash per bale, respectively. The seed cotton is transported to the gin where the ginning process separates the trash from the cotton, and the cotton gin trash (CGT) is accumulated at the gin. Every season, gins accumulate thousands of tons of CGT (fig. 1).

Figure 1. Image of cotton gin trash.

In most cases, CGT is viewed as a waste product that has to be properly collected and removed from the ginning site. Since the trash is a biomass with an energy content of approximately 16.3 MJ kg^{-1}, gins can convert the energy from the trash to usable energy. Initially, combustion systems were developed in which the product heat could be used directly for drying the cotton or for steam production. Combustion of CGT in furnace systems were used for drying with air to air heat exchangers, however after a short duration of time, the operation becomes unsustainable. The high temperatures (>1100°C) of combustion surpass the eutectic point of the ash in the CGT, resulting in slagging and fouling. The melted ash deposits and adheres to the inner surfaces of the combustion system.

To investigate the problems of slagging and fouling, an atmospheric fluidized bed combustion unit was developed by Lepori et. al. (1981) at Texas A&M University. The unit was a 61 cm (2 ft) diameter reactor with refractory sand as the bed material. Tests involved feeding CGT with a screw conveyor into the combustion unit. The CGT was combusted at temperatures near 760°C. After the tests, layers of the ash and fouling deposits were found on the surfaces of the unit. A chemical composition analysis was conducted that revealed the metallic compounds (ash content) of the biomass accumulated on the surfaces. High corrosion and erosion rates were observed on the low carbon steel surfaces. A portion of the ash had also melted and adhered to the bed material particles, causing the bed to become agglomerated. The conclusion from the study was that the CGT was a high-slagging and high-fouling fuel.

An alternative approach for energy conversion from the CGT was then experimented through fluidized bed gasification (FBG). The gasification process can be controlled to operate at temperatures that are below the eutectic point of the ash, reducing slagging and fouling. Gasification's primary product is a low calorific value combustible synthesis gas, also known as syngas. Instead of capturing heat for direct use, Lepori and Egg (1994) developed a FBG steam producing system fueled by CGT. The syngas generated from the 610 mm diameter reactor was combusted in a fire tube boiler to produce steam. The study determined the production rate of steam and overall energy conversion efficiency based on the CGT feed rate. The steam production from the system could be used to estimate potential electrical power if a steam turbine generator were to have been implemented.

Although the FBG steam producing system showed promise for electricity generation, implementing such a system was not economically viable. A high cost was associated with the steam power cycle, along with the large amounts of water needed (Capareda, 2014). Therefore, instead of producing steam from gasification, the syngas was suggested to be directly combusted in an internal combustion engine to power a generator to generate electricity. Maglinao (2013) operated a gasoline generator fueled by syngas from FBG at Texas A&M University. The fuel used for gasification was municipal solid waste (MSW). The overall biomass (MSW) to electricity conversion efficiency from the generator tests ranged between 7% and 20%, which can be expected to be similar for other biomass fuels, such as CGT.

On average, cotton gins utilize approximately 50 kWh of electricity to gin a bale of cotton (TCGA, 2006). The total amount of electricity that a gin requires can be predicted by the gin's rating. A power analysis (fig. 2) for gins was performed assuming that 10% of the energy in the CGT can be converted to electricity through FBG. The analysis revealed that for a 20, 40, and 60 bale per hour gin, the required power to operate the gin was 1, 2, and 3 MW, respectively. The stripper gins contained more than enough CGT to meet the gin's power demand, whereas the picked gins could only be partially self-sustaining. In reality, however, gins receive seed cotton that is both picked and stripped. In most cases, gins pay for the disposal of the CGT. Since the CGT is located on site at the gin, the biomass fuel is readily available for energy conversion.

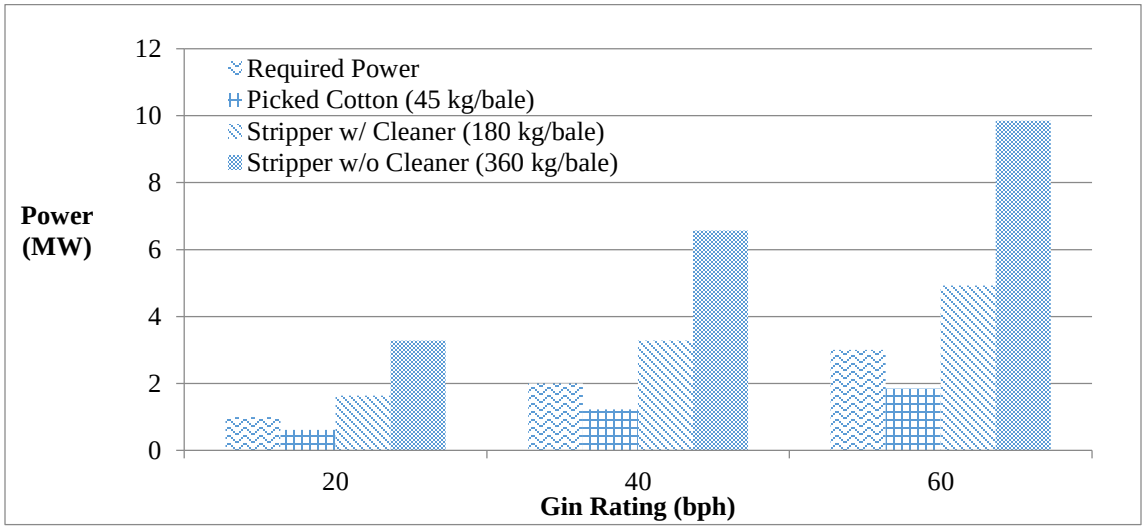

Figure 2. Analysis of power generation utilizing cotton gin trash.

Since the ginning season only lasts around three months out of the year, the reality is that the gin will not use the CGT to power the gin during the season, but rather gasify the waste biomass during the offseason to generate electricity. The generated electricity can be sold back to the power grid through net metering. To qualify for net metering, the electricity being sold to the grid can be generated only from wind, solar, or waste biomass. Since CGT is a waste biomass byproduct, cotton gins would be accepted for the net metering option in which the gin would generate revenue by selling electricity back to the grid.

Lummus Corporation has partnered with the Department of Biological and Agricultural Engineering at Texas A&M University to make the step forward of developing a sustainable FBG for electricity generation at a cotton gin. The objective of this project was to design a system (fig. 3) that could produce 500 kW of electricity fueled by CGT. To achieve the objective, a pilot scale gasification system was used and tested to develop the engineering properties for the scaled up design. The pilot scale system, compared to a larger system, is much simpler to control and operate while reducing the amount of fuel used to run experiments.

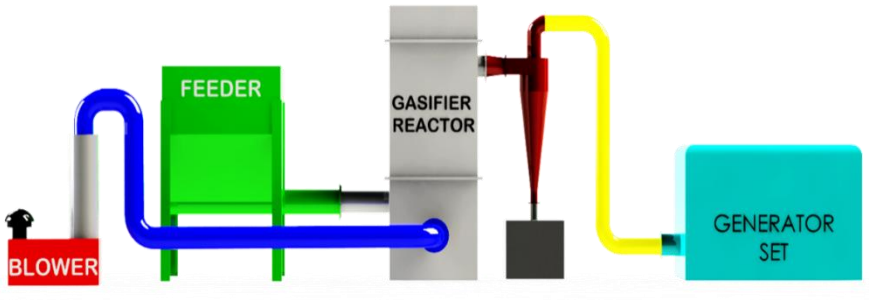

Figure 3. Basic components of a fluidized bed gasification system for electricity generation.

Each component of the FBG system needed to be designed and operated properly to achieve a sustainable and continuous generation of electricity. For this project, three major areas of the FBG system were investigated to achieve the overall objective: 1) minimum fluidization of the bed material in the reactor, 2) cyclone performance for biochar capture, and 3) determining the optimum operating parameters of the gasifier for continuous and sustainable electricity generation. Each of these aspects were crucial for the system to produce the desired electrical output sustainably.

Research Objectives

The objective of the research was to experimentally determine the operating parameters of a pilot scale gasifier that can be used as an engineering design basis to scale the gasification system up to generate 500 kW of electricity.

Specific objectives of this research were as follows:

1) determine and evaluate an appropriate method that accurately predicted the minimum fluidizing velocity of the bed material,

2) determine the location of the vortex inverter within the tube cyclone that achieved the highest capture efficiency of biochar, and
3) determine an optimum combination of energy loading and fuel-to-air ratio of the pilot scale gasifier that resulted in a sustainable and continuous operation capable of generating electricity.

CHAPTER II

MINIMUM FLUIDIZING VELOCITY

Introduction

The fluidization of the bed material plays an underlying vital role in the fluidized bed gasification process. The fluidization of the bed material not only serves as the media to gasify the biomass, but allows the operation to be carried out in a continuous manner. Once the bed material has been fluidized and heated to the temperatures of gasification, the bed media becomes a near isothermal region that provides for an excellent transfer of heat to the biomass (Lepori and Soltes, 1985). The thermal energy in the bed material transfers to the biomass through the agitation of the fluidized bed particles. Since there is a controlled amount of air supplied to the bed, which is approximately 79% nitrogen and 21% oxygen, all of the oxygen is consumed and reacted with a fraction of the biomass to sustain the temperature of the bed. As a result, the fluidized bed for gasification makes this method a more continuous process, straying from the conventional batch type processes.

To fluidize the bed material in a reactor for fluidized bed gasification (FBG), air needs to flow upwards through the material. Bed material typically consists of a refractory sand able to withstand the high temperatures of gasification. The superficial velocity of the air at which the bed material first exhibits fluid-like behavior is said to be the minimum fluidization velocity (MFV). At the onset of fluidization, the air just suspends the particles; the upward drag force of the air is equal to the weight of the

particles. Both the properties of the air and the bed material needed to be determined to accurately predict the MFV. Properties of the bed material include the mean particle diameter, particle density, sphericity, and voidage. Properties of the air are the density and viscosity, both dependent on the temperature.

A method that accurately predicted the MFV was needed to properly control the state of the bed material during gasification. If the velocity of the air was not sufficient to fluidize the bed, then the bed was said to be static, in which gasification would not occur. The static bed would not uniformly distribute the heat to the biomass and the biomass would only accumulate in the chamber. If the velocity of the air was too high, bed material particles would elutriate out of the reactor at a rate that would eventually deplete all particles. Without bed material, there would not be media to transfer the thermal energy to the biomass for gasification. Therefore, there was a window of superficial velocities through the bed material that resulted in a sustainable process for gasification.

A common method used to predict the MFV is a model developed by Kunii and Levenspiel (1991), which is presented later in this chapter. The model takes into account the properties of the bed material and the fluidizing air, setting the weight of the particles equal to the drag force of the air and yields the theoretical MFV of the bed material. To ensure the theoretical MFV was accurate, an experimental set up was required to determine the actual MFV of the bed material. However, the actual MFV could only be determined from ambient air tests, rather than air at the hot temperatures of gasification. The pilot scale gasifier, which could be used to heat the air and bed material to a high

temperature, did not have pressure taps in the appropriate locations to measure the pressure drop across the bed. Therefore, a chamber similar to that of the gasifier was used to determine the actual MFV of the bed material. The actual MFV was compared to the theoretical MFV at ambient conditions to determine the accuracy of the model. If the model accurately predicted the MFV at ambient conditions with a small margin of error, then the assumption was made that the equation accurately predicted the MFV at the temperatures of gasification.

Determining the actual MFV at ambient conditions was achieved by plotting the superficial velocity of air through the chamber with the pressure drop through the bed material, as seen in the ideal plot in figure 4. As the superficial velocity of the air increases, the pressure drop across the static bed (OA region) also increases in a near linear relationship. The particles of the bed material in a static bed do not move relative to one another. Once the bed becomes fluidized (BC region), the pressure drop becomes constant with increasing air velocity. Before the bed becomes fluidized, an extra force is generally required by the air to overcome the static friction of the particles of the bed (point A). The velocity of air at this point is defined as the MFV (V_{mf}).

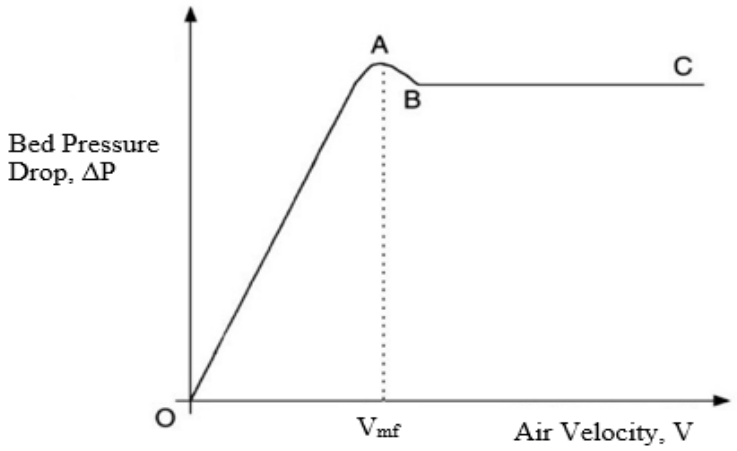

Figure 4. Bed pressure drop vs. superficial velocity. Point A is defined as the point where the bed first becomes fluidized. Reprinted with permission from Rhodes (2008).

Materials and Methods

The bed material used for the fluidization tests was MULCOA 47 (C-E Minerals, King of Prussia, Pa.), which has a reported particle density ($\rho_{particle}$) of 2.6 g cm^{-3}. The particle size analysis of the refractory sand was carried out by a Ro-Tap Test Sieve Shaker model RX-89 (Ro-Tap, Mentor, Ohio) that determined the mass fraction of particles in certain size ranges. Test sieves with mesh sizes of 250, 297, 355, 500, and 1000 µm were used to determine the size ranges. From the particle size analysis, the mean particle size ($\bar{d}_p$) of the bed material was calculated by using equation 1.

$$\bar{d}_p = \frac{1}{\sum_{all\ i} (x/d_p)_i} \quad (1)$$

where
$\bar{d}_p$= mean particle size (cm)
x = weight fraction within a certain sieve size range (dimensionless)
d_p = average particle size within a certain sieve size range (cm).

Ambient air fluidization tests were conducted with a 0.15 m (6 in.) diameter Plexiglass chamber (fig. 5) that was set up similar to that of the gasifier unit. Air was supplied by a Sutorbilt type L positive displacement compressor (Gardner Denver, Quincy, Illinois) connected to a Fuji Electric type FRN005C1S-2U variable AC controller (Tokyo, Japan). The flow rate of air was determined by measuring the pressure drop across an inlet orifice meter. The Plexiglass chamber had multiple pressure taps vertically on the surface so that the pressure drop across the bed could be measured at different heights of bed material. All pressures were measured by Magnehelic gauges.

Figure 5. Plexiglass chamber for minimum fluidization tests of the bed material.

Fluidization tests were conducted by varying the flow rate of the air through the Plexiglass chamber. The flow rate was converted to a superficial velocity since the cross

sectional area of the chamber was known. The pressure drop across the bed was measured at each flow rate to develop a pressure drop versus superficial velocity curve. The MFV for each test was determined at the point where the pressure drop across the bed first became constant. The MFVs determined from the curves were used to validate the MFV equation (eq. 2) at ambient conditions (Kunii and Levenspiel, 1991).

$$V_{mf} = \frac{\bar{d}_p{}^2 \cdot (\rho_p - \rho_a) \cdot g}{150 \cdot \mu} \cdot \frac{\varepsilon^3 \cdot \Phi^2}{1-\varepsilon} \quad (2)$$

where
V_{mf} = minimum fluidization velocity (cm s^{-1})
$\bar{d}_p$ = mean diameter particle (cm)
ρ_p = particle density (g cm^{-3})
ρ_a = air density (g cm^{-3})
g = gravity acceleration (cm s^{-2})
ε_{mf} = bed voidage at minimum fluidization (dimensionless)
φ = sphericity (dimensionless)
μ = air viscosity at operating temperatures (g cm^{-1} s^{-1}).

The sphericity (Φ) is defined as the ratio of the surface area of a sphere to the surface area of an irregularly shaped particle having the same volume as that of the sphere. Reported values of sphericity for sharp and round sand are 0.67 and 0.86, respectively (Kunii and Levenspiel, 1991). Therefore, when calculating the MFV with equation 2, an average sphericity value of 0.77 was used.

The bed voidage at minimum fluidization was calculated at the point of initial fluidization. At the onset of fluidization, the bed height slightly increases. This bed height was recorded to calculate the bulk density at fluidization by determining the volume. The mass of bed material was weighed before being inserted into the chamber. Thus, the bed voidage at minimum fluidization was determined by equation 3.

$$\varepsilon_{mf} = 1 - \frac{\rho_{bulk}}{\rho_{particle}} \quad (3)$$

where
ε_{mf} = bed voidage at minimum fluidization (unitless)
ρ_{bulk} = bulk density at fluidization (g cm^{-1})
$\rho_{particle}$ = particle density (g cm^{-1}).

The properties of ambient air were obtained by an Ambient Weather model WS-1171A weather station (Chandler, Ariz.) to calculate the density. The properties reported were the barometric pressure, relative humidity, and temperature. Equation 4 was applied to calculate the density of air.

$$\rho_a = \left(\frac{P_b - (\phi * P_s)}{0.0028 * (t_{db} + 273)} + \frac{\phi * P_s}{0.0046 * (t_{db} + 273)}\right) * 0.001 \quad (4)$$

where
P_b = abs. barometric pressure (atm)
ϕ = relative humidity ratio (decimal form)
P_s = abs.saturation pressure of water vapor at dry bulb temp. (atm)
t_{db} = dry bulb temperature (°C).

The height of the bed material when operating the pilot scale gasifier was approximately 0.3 m (12 in.). This height was selected to be the median when testing the MFV in the Plexiglass chamber. Three heights of bed material were selected for the MFV tests, which were 0.2, 0.3, and 0.4 m. An adhesive measuring tape was placed vertically on the surface of the Plexiglass chamber to record the initial height and the height of the bed at the onset of fluidization. Three tests were ran for each bed height and the average MFV from all nine tests was compared to the theoretical MFV from equation 2 by calculating the percent error.

Results and Discussion

The bed mean particle size of the refractory sand was calculated to be 818 µm by taking an average of three tests, as seen in table 1. From all three tests, an average of 39% of the particles were greater than 1000 µm, 60% of the particles fell between the 500 and 1000 µm range, and the remaining 1% of particles were between 250 and 500 µm.

Table 1. Average mean particle size of bed material from three particle size distribution tests.

Test	Mean Particle Size (µm)
1	832
2	803
3	819
Average	**818**

The pressure drop across the bed versus the superficial velocity plot was used to determine the MFV for each test. An example plot is shown in figure 6. The plots developed from the nine MFV tests displayed the same characteristics of the ideal plot (fig. 4). A near-linear relationship was observed between superficial velocity and the pressure drop across the static bed. The bed had reached fluidization once the pressure drop became constant with increasing velocity.

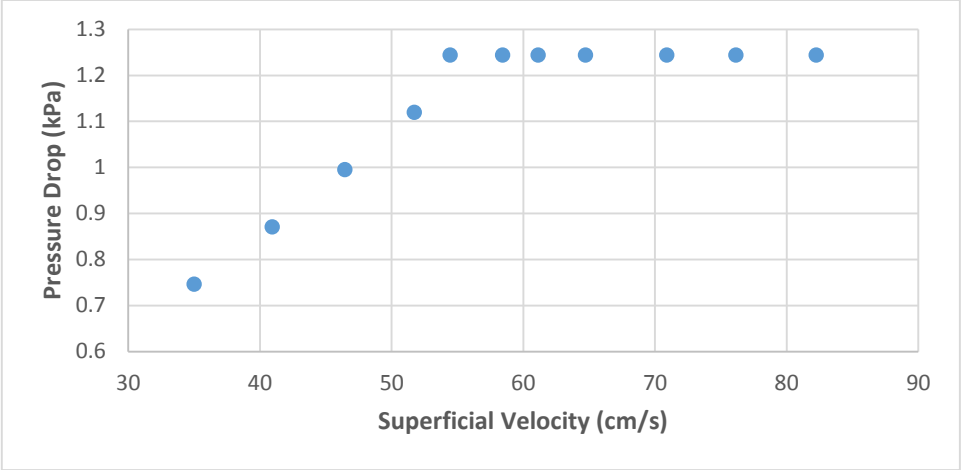

Figure 6. Pressure drop vs. velocity plot for bed material at 0.3 m.

A summary of the results for the MFVs are shown in table 2. The average bed voidage at the MFV (ε_{mf}) was 0.46. The measured MFV from all tests ranged between 54.4 and 57.4 cm s^{-1}, while the average was 56.0 cm s^{-1}. The theoretical MFV from equation 2 yielded a value of 63.5 cm s^{-1} at the same conditions as the ambient tests. The percent error between the average actual MFV and the theoretical MFV was 11.8%. The density and viscosity of air at the ambient conditions of testing were found to be 1.2 kg m^{-3} and 1.83 x 10^{-5} kg m^{-1} s^{-1}, respectively.

Table 2. Measured minimum fluidizing velocities of the bed material at different heights.

Bed Height [m]	Measured Minimum Fluidization Velocity [cm s^{-1}]
0.2	56.4
0.2	56.4
0.2	56.4
0.3	54.4
0.3	54.4
0.3	54.9
0.4	56.9
0.4	57.4
0.4	56.9

When running the MFV experiments, data was recorded from the Magnehelic pressure gauges. Due to the nature of the experimental set up, the pressure gauges would display slight fluctuating pressures (± 0.25 kPa) at constant conditions, such as flow rate. This was a consequence of using a positive displacement compressor, which supplies air in a pulsing manner. The pressure determined for each data point was calculated by averaging the highest and lowest observed pressures displayed by the gauge. The fluctuating pressures accounts for some error in the measured MFV from the tests.

Applying equation 2 to predict the MFV at the operating conditions of the gasifier yielded a value of 30.7 cm s^{-1}. The temperature of the air was assumed to be 650°C, which correlated to a predicted density and viscosity of 0.38 kg m^{-3} and 3.95 x 10^{-5} kg m^{-1} s^{-1},respectively. Intuitively, the MFV would increase at higher temperatures of air, since the less dense air has less mass to apply a drag force against the bed particles. The MFV at the operating conditions is slightly less than one-half of the MFV

at ambient conditions. Kunii and Levenspiel (1991) summarized from other researchers that the lower MFV at higher temperatures was being observed.

When conducting the MFV tests, observations were made to visually characterize the bed as it was being fluidized. The point at which the bed becomes fluidized was when small air bubbles formed at the base of the chamber and traveled upwards. As the velocity of air through the chamber was increased, the size of the bubbles also increased. Once the bubbles reached the top of the bed material's surface, they would "pop" and throw up bed material into the freeboard. The amount of bed material being thrown up was observed to be dependent on the size of the bubbles. Thus, as the air velocity increased, the height and amount of bed material being thrown up also increased.
An attempt was made to find a correlation between height of thrown up bed material and air velocity to aid in the design of the freeboard of the larger gasifier's reaction chamber. However, the height of thrown up bed material was inconsistent at steady air velocities. This was due to how the air bubbles traveled and coalesced through the bed.

Summary and Conclusions

The particle size distribution (PSD) of the bed material particles was determined by calculating the mass fraction of particles in certain size ranges. The sieves used to determine the size ranges had mesh sizes of 250, 297, 355, 500, and 1000 µm. The mean particle diameter of the bed material was calculated to be 818 µm.

Ambient air fluidization tests were conducted in a Plexiglass chamber that was set up similar to the pilot scale gasifier. The minimum fluidization velocity (MFV) of the

bed material was experimentally determined by locating the point where the bed first experiences a constant pressure drop. Three tests were ran at each bed height of 0.2, 0.3, and 0.4 m to determine the overall average MFV. The average experimental and calculated theoretical MFV was 56.0 and 63.5 cm s^{-1}, respectively.

The percent error between the actual and theoretical MFV values at ambient conditions was 11.8%. Although the percent error was above 10%, equation 2 over predicted the MFV of the bed material. The conclusion was drawn that equation 2 can be used to predict the MFV of the bed material during the hot, operating conditions of the gasifier.

CHAPTER III

TUBE CYCLONE PERFORMANCE

Introduction

A byproduct from the gasification of biomass is biochar. Biochar is an ash-like particulate discovered to be activated carbon (Capareda, 1990). An important aspect in the gasification process is the removal of biochar from the syngas before the gas is combusted in an internal combustion engine (ICE) (Maglinao, 2013). Typical gasification systems utilize cyclones to separate the biochar from the syngas (Lepori et al, 1985). Cyclones are excellent particle abatement devices that are capable of achieving 90% and above capture efficiency. In addition, cyclones are relatively inexpensive to manufacture, have very few maintenance requirements, and have low operation costs (Cooper and Alley, 2011, pp. 136).

A gas containing the particulate enters the inlet of the cyclone (fig. 7) tangentially to the barrel of the cyclone. The gas stream spirals downward in the cyclone (outer vortex) using centrifugal forces to move the particles to the surface of the cyclone, where the particles will slide down and be captured. At the natural length of the cyclone near the bottom of the conical section, the outer vortex changes direction and gets inverted to the inner vortex. The inner vortex then travels upward through the center of the cyclone to the outlet.

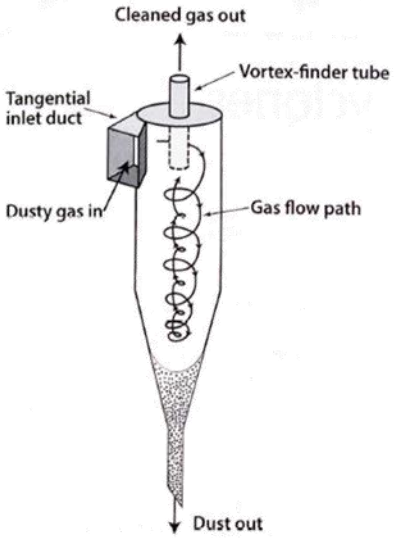

Figure 7. Basic operation of a cyclone for particulate capture.

The early stages of the FBG system at Texas A&M University utilized a two-stage cyclone clean-up system (LePori and Parnell, 1983). The clean-up system had a 1D3D cyclone followed by a 1D5D cyclone in series. The 1D3D cyclone had the function to capture the larger biochar particles, whereas the 1D5D cyclone would capture the finer particles. The capture efficiencies were recorded for both cyclones as the FBG system was operated. The 1D3D cyclone had capture efficiencies ranging between 90% and 95%, but the 1D5D cyclone only increased the overall efficiency by no more than 5%.

Saucier (2013) set up a similar apparatus but instead had a 1D2D cyclone followed by a 1D3D cyclone for biochar captured. The system was tested at ambient conditions and achieved an overall capture efficiency of 97% and higher, but it was observed that a

majority of the biochar was captured by the 1D2D cyclone. A separate test was conducted to determine the capture efficiencies of the cyclones individually. The reported capture efficiencies of the 1D2D and 1D3D cyclones were approximately 97% for both. Since the 1D2D cyclone was capturing a majority of the particulate, a second cyclone would only increase the overall efficiency by 1% to 3%. The overall conclusion was that only one cyclone would suffice for the separation of biochar from the syngas.

An important aspect to achieving a high capture efficiency is the proper design of the cyclone. Hoffmann (1995) reported that the natural length of the cyclone increased with increasing inlet velocity. The physical length of the cyclone needs to be at or below the natural length to achieve a high capture efficiency. If the physical length of the cyclone is less than the natural length, the outer vortex strands intermix. The outer vortex does not transition to the inner vortex smoothly, and a turbulent region within the cyclone is created. The result of the turbulent region decreases the overall efficiency of the cyclone.

When the FBG is operated, both the temperature and the flow rate of the syngas entering the cyclone vary. The natural length of the cyclone is affected by the flow rate. Luehrs (2014) tested the performance of a Plexiglass tube cyclone with a vortex inverter at ambient conditions to simulate the variation of the temperature of the gases from the gasifier. Three temperatures were selected: 20°C, 278°C, and 554°C. Each correlated to a flow rate of gases, which, in turn, correlated to an inlet velocity to the cyclone. The natural length was calculated based on the inlet velocity and was the location of the vortex inverter. The vortex inverter was used to invert the outer vortex to the inner vortex in the tube cyclone. The position of the vortex inverter was measured in terms of

cyclone diameter (D) below the inlet. Vortex inverter positions of 4D, 6D, and 8D correlated to an inlet velocity of 16.3, 30.5, and 45.7 m s^{-1} (3200, 6000, and 9000 ft min^{-1}), respectively. The reported capture efficiencies of the tube cyclone for each vortex inverter position ranged between approximately 96% and 98%. Luehrs concluded that the vortex inverter should be placed just below the natural length to achieve the high capture efficiency, where the natural length is calculated by the expected flow rate of gases.

For the current research project, a stainless steel tube cyclone was used to separate the biochar from the syngas. The tube cyclone (fig. 8) was expected to achieve a high capture efficiency of biochar, regardless of the variation of flow rates from the gasification process. Ambient tests were conducted to determine the natural length of the tube cyclone, which was where the vortex inverter was located within the cyclone that achieved the highest capture efficiency. The location of the vortex inverter determined from the ambient tests would be used for the cyclone when operating the gasifier to clean the syngas.

Figure 8. Tube cyclone (left) and vortex inverter (right).

Materials and Methods

The tube cyclone was designed using the Texas A&M cyclone design (TCD) method for a 1D3D cyclone. Preliminary calculations by Luehrs (2014) revealed an estimated volumetric flow rate of 0.71 Nm^3 min^{-1} of gases from the 0.15 m diameter gasifier. With a design inlet velocity of 975 m min^{-1}, the inlet area of the cyclone was calculated by dividing the flow rate by the inlet velocity. The inlet area was then used to calculate the diameter of the cyclone (eq. 5).

$$A_{inlet} = \frac{D^2}{8} \quad (5)$$

where
A_{inlet} = inlet area of cyclone (m^2)
D = diameter of cyclone (m).

Equation 5 is derived from the length and width of the 1D3D cyclone inlet, which are D/2 and D/4, respectively. The diameter of the tube cyclone was calculated to

determine the inlet and outlet dimensions. The length of the tube cyclone was sized to allow sufficient variation of the vortex inverter position when testing cyclone performance, up to 10D. All parts of the cyclone were constructed of stainless steel by Lummus Corp. to withstand the elevated temperatures of gasification.

Biochar from past gasification tests was the particulate used when testing the performance of the tube cyclone at ambient conditions. The particle size distribution (PSDs) of the input biochar was obtained with a Beckman Coulter Counter Multisizer 3 (Beckman Coulter, Miami, Fla.). The analysis determined the best fit mass mean diameter (MMD) and geometric standard deviation (GSD) of the biochar samples. The MMD of the biochar samples from the Coulter Counter were reported as equivalent spherical diameter (ESD) and converted to aerodynamic equivalent diameter (AED). The particles analyzed were between 2 and 100 μm due to Coulter counter limitations. The particle density of the biochar was calculated in part by a Multipycnometer model MVP 4AC232 (Quantachrome, Boynton Beach, Fla.).

The feeding of the biochar was achieved by using a feed hopper and a variable speed rotary air lock apparatus. A 5 cm diameter plastic smooth wall hose was used to connect the T-section to the inlet of the cyclone. Figure 9 shows a schematic of the system that was used to evaluate the performance of the cyclone.

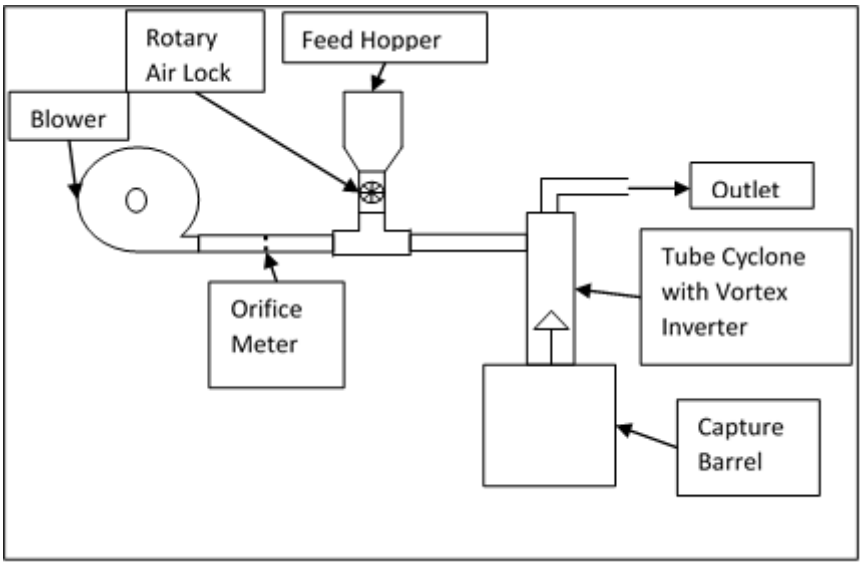

Figure 9. Schematic of cyclone testing.

Cyclone performance was evaluated by determining capture efficiency using air at ambient conditions. This was done by calculating the ratio of captured to input biochar by mass. The masses were recorded with a Doran Scales model PC-400 digital scale (Doran Scales, Inc., Batavia, Ill.). The vortex inverter position was varied between each test run at positions of 4D, 6D, 8D, and 10D (fig. 10). Each position is an increment of cyclone diameter that was measured from the bottom of the inlet of the cyclone to the base of the vortex inverter.

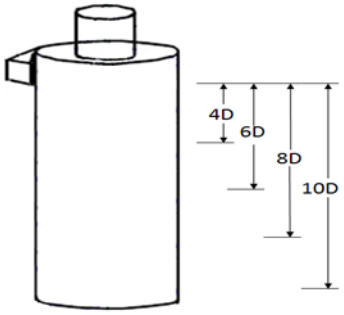

Figure 10. Vortex inverter positions within tube cyclone (not to scale).

For each vortex inverter position, two flow rates of 1 and 1.4 m^3 min^{-1} were used when testing the performance of the cyclone as these were the estimated actual flow rates when operating the gasifier. The flow rates of 1 and 1.4 m^3 min^{-1} equated to a cyclone inlet velocity of 1370 and 1950 m min^{-1}, respectively. Two replicates were performed for each vortex inverter position and flow rate. The response of each test run was the capture efficiency of the cyclone. The assumption was made that the temperature and density of gas conveying particulate did not affect the performance of the cyclone. Therefore, the capture efficiencies of the tube cyclone at ambient conditions can be expected to be similar during gasification.

The results of the tube cyclone tests were statistically analyzed by Design-Expert 9 (Stat-Ease, Minneapolis, MN). The experiments were randomized and blocked by replicate. An analysis of variance (ANOVA) test was conducted to determine if the factors (flow rate and vortex inverter position) affected the result (capture efficiency). The significance level selected was 5%, therefore, the factors were deemed significant if the calculated p-value was less than 0.05.

Results and Discussion

The PSD of the biochar obtained from the Coulter Beckman Multisizer 3 revealed a best fit MMD of 24 µm (AED) with a GSD of 1.8 (fig. 11). The particle density was 2.1 g cm^{-3}.

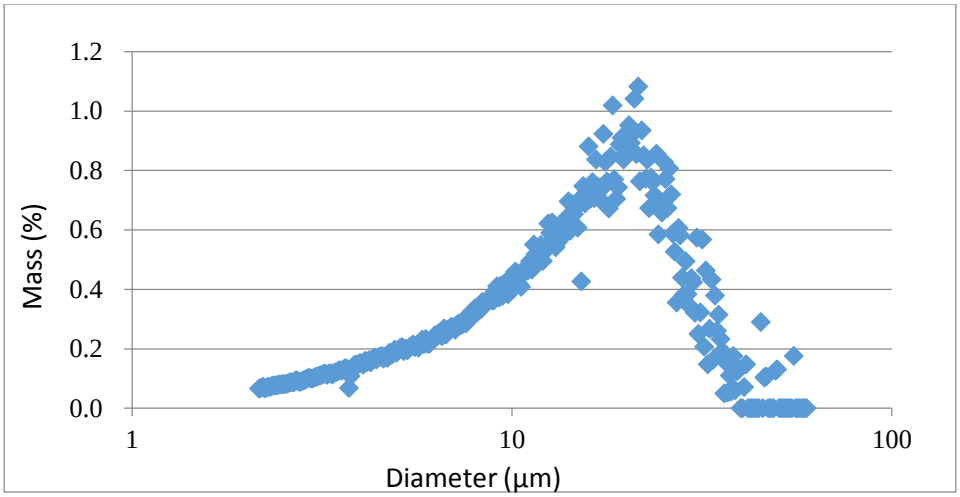

Figure 11. PSD of biochar sample used for cyclone testing.

A total of 16 experiments were run to determine the capture efficiency of the tube cyclone by varying flow rate and vortex inverter position. Each run had a testing time of approximately 6 minutes. The average concentration of biochar for flow rates of 1 and 1.4 m^3 min^{-1} were approximately 100 and 70 g m^{-3}, respectively.

The capture efficiencies of the cyclone ranged between 95.0% and 99.1%. A visual representation (fig. 12) reveals a near horizontal relationship between vortex inverter position, flow rate, and capture efficiency of the tube cyclone. This horizontal

relationship signifies that vortex inverter positions between 4D and 10D, and flow rates between 1 and 1.4 m^3 min^{-1}, have an insignificant effect on the capture efficiency.

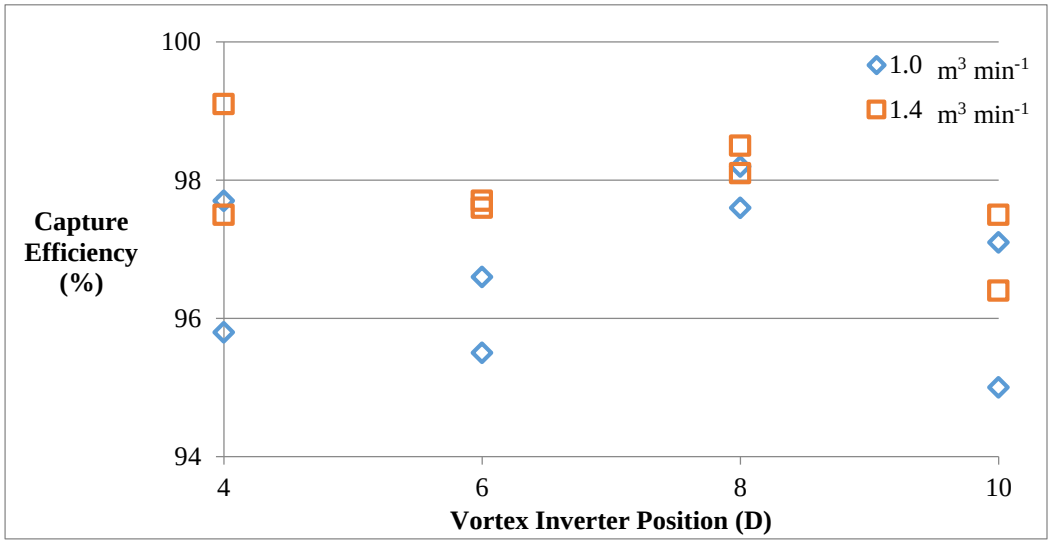

Figure 12. Plot of tube cyclone capture efficiency results by varying vortex inverter position and flow rate.

The results of the ANOVA test by Design Expert 9 revealed that, between the tested variables, both the vortex inverter position and the flow rate had an insignificant effect on the capture efficiency (table 3). The p-value for the vortex inverter position and the flow rate were 0.188 and 0.058, respectively. Although the flow rate was deemed statistically insignificant, the capture efficiency was in some cases greater at a flow rate of 1.4 m^3 min^{-1}, by up to approximately 3%.

Table 3. Analysis of variance results for determining the effect of vortex inverter position and flow rate on the capture efficiency.

Factor	Sum of Squares	df	Mean Square	F value	p-value
Vortex Inverter	6.08	3	2.03	2.11	0.188
Flow Rate	4.95	1	4.95	5.15	0.058

To confirm that the vortex inverter had an insignificant effect on the capture efficiency, additional tests were ran without the vortex inverter. At flow rates of 1 and 1.4 m^3 min^{-1}, without the vortex inverter, the capture efficiencies of the tube cyclone ranged between 96% and 98%. Therefore, it was concluded that the tube cyclone would achieve above 95% capture efficiency of biochar during gasification without the vortex inverter.

Summary and Conclusions

A tube cyclone was designed using the Texas A&M cyclone design (TCD) method for a 1D3D cyclone. Ambient air tests were conducted to evaluate the capture efficiency of biochar by varying the flow rate of air and the vortex inverter position within the cyclone. The PSD of the biochar particulate revealed a best fit MMD and GSD of 24 µm (AED) and 1.8, respectively. The particle density was calculated to be 2.1 g cm^{-3}.

Capture efficiencies of the tube cyclone at ambient conditions ranged between 95% and 99%. The vortex inverter positions between 4D and 10D, and flow rates between 1 and 1.4 m^3 min^{-1}, were determined to have a statistically insignificant effect on the capture efficiency. Additional tests were ran to determine the capture efficiency

of the cyclone by removing the vortex inverter. Without the vortex inverter, at flow rates of 1 and 1.4 m^3 min^{-1}, the capture efficiency was between 96% and 98%.

CHAPTER IV

FLUIDIZED BED GASIFICATION

Introduction

Gasification is a thermo-chemical conversion process that converts a biomass to a low calorific value (LCV) combustible gas, also known as syngas. The gasification process occurs in an oxygen-deprived environment at elevated temperatures, generally ranging between 750°C and 850°C (Capareda, 2014). When a controlled amount of air is introduced into the gasifier, the oxygen in the air reacts with the carbon in the biomass (combustion) to produce carbon dioxide gas and heat (eq. 6). Since there is a controlled amount of air entering the gasifier, only a portion of the carbon in the biomass is being utilized to generate heat. This means that a portion of the biomass fuel is used to sustain the temperature of the reaction. The carbon dioxide gas reacts with the carbon in the biomass to produce carbon monoxide gas. This reaction is commonly known as the Boudouard reaction (eq. 7). The water in the biomass and air react with carbon in the biomass to form carbon monoxide and hydrogen gas, known as the water-gas shift reaction (eq. 8).

$$C + O_2 \rightarrow CO_2 + \text{Heat} \quad (6)$$

$$CO_2 + C \rightarrow CO \quad (7)$$

$$H_2O + C \rightarrow CO + H_2 \quad (8)$$

In addition to carbon monoxide and hydrogen gas being formed during gasification, other combustible gases are generated. These include methane, ethylene, and other hydrocarbons (Lepori and Soltes, 1985).

For fluidized bed gasification (FBG), a fluidized bed reactor (fig. 13) is used to carry out the process. A chamber is partially filled with a bed material, typically comprised of refractory sand, in which a controlled amount of air is introduced from the bottom. The air travels upwards through the bed material with such a velocity that will fluidize the bed. The bed is said to be fluidized once the bed material particles exhibit fluid-like behavior. The fluidization of the bed material provides for a near isothermal, turbulent region during the gasification process.

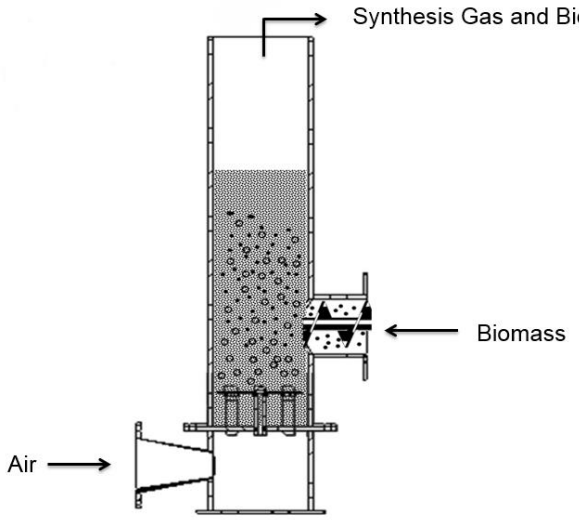

Figure 13. Basic principle of a fluidized bed reactor for gasification.

To ensure the FBG operation is sustainable and continuous, the feed rate of the biomass fuel and air flow rate need to be properly monitored and controlled. The two operational parameters that are crucial to the control of the gasification process are the energy loading (EL) and the fuel to air (F/A) ratio. The EL is a function of the feed rate of the biomass per cross sectional area, and has units of GJ h^{-1} m^{-2}. The F/A ratio is the ratio of the rate of input biomass to input air, expressed as kg_{fuel}/kg_{air}.

The primary product of FBG is the syngas. The quality of the syngas is based on its lower heating value (LHV). Typical LHVs of syngas produced from the gasification of cotton gin trash range between 4 and 5 MJ Nm^{-3} (Maglinao, 2013). The production and quality of the syngas is dependent upon both the EL and F/A ratio. Both the EL and the F/A ratio can be varied experimentally to determine a sufficient quality of syngas and energy conversion efficiency to sustainably generate electricity.

The temperature of the gasification reaction is also dependent upon the operational parameters. A key advantage of FBG is the ability to properly control the reaction temperature. The main component that affects temperature is the F/A ratio; an increase in the F/A ratio results in a decrease in the reaction temperature (Capareda, 2014). The temperature plays a key role in the sustainability of the process. Temperatures that go above the eutectic point of the biomass and the melting point of the ash result in slagging and fouling, causing blockage in the system. Bed agglomeration has also been observed in fluidized bed reactors (Olofsson et. al., 2002) in which the melted ash of the biomass causes the bed particles to adhere to one another.

Once a combination of EL and F/A ratio have been determined, the validation of electricity generation can be demonstrated by continuously directing syngas to an ICE. The combination of EL and F/A ratio that result in sustainable electricity generation can be used as the design parameters for scaling the FBG system up to generate a desired electrical output, such as 500 kW.

Materials and Methods

The pilot scale gasifier that was used throughout this project was a 0.15 m (6 in.) diameter cylindrical stainless steel tube. Figure 14 illustrates the flow diagram of the operation of the FBG system. Air was supplied by a Sutorbilt type L positive displacement compressor connected to a Fuji Electric type FRN005C1S-2U variable AC controller. The flow rate of the ambient air was measured by an inlet orifice meter. Prior to gasification, a propane burner heated the bed material to temperatures above 538°C. Once this temperature had been reached, the propane burner was turned off and the biomass fuel fed into the gasifier through a screw conveyor. The syngas and biochar reactants were conveyed out of the gasifier outlet and to the tube cyclone. The cyclone partially separated the biochar from the syngas and the biochar collected in the capture barrel. The syngas exited the cyclone outlet and passed through the venturi meter, where the volumetric flow rate was measured. The syngas was then directed at the T-section to either be flared off or combusted in the engine in the generator.

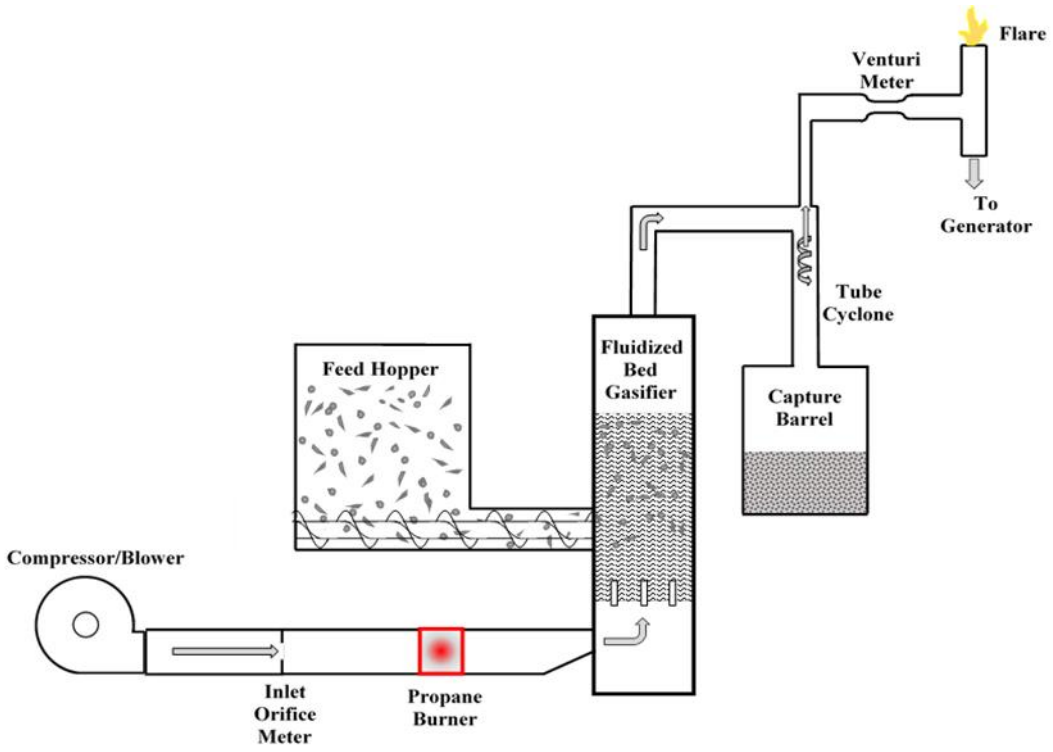

Figure 14. Flow diagram of the 0.15 m diameter fluidized bed gasification system.

Several measurements were taken periodically during operation, every 5 to 10 minutes. Temperatures were obtained by thermocouples and measured at the inlet orifice meter, lower bed material, upper bed material, inlet of the cyclone, and inlet of the venturi meter. Differential pressures were measured by Magnehelic gauges at the inlet orifice meter, bed material, gasifier unit, cyclone, and venturi meter. Static pressures were measured at the lower bed material, upper bed material, and at the inlet of the venturi meter. A gas sample port was implemented into the system downstream of the venturi meter to extract samples of syngas during operation. The samples were analyzed with an SRI Instruments gas chromatograph model 310C (Torrance, Cal.) in which the

components of the gas were reported, by volume, and the lower heating value of the syngas was calculated (eq. 9).

$$LHV_s = \frac{\sum(V_i \cdot LHV_i)}{100} \quad (9)$$

where
LHV_s = lower heating value of gas sample (MJ Nm^{-3})
V_i = volume of gas component (%)
LHV_i = lower heating value of gas component (MJ Nm^{-3}).

Milo (grain sorghum) was used as the biomass fuel in this study since it can be uniformly fed into the 0.15 m diameter gasifier. In addition, milo was a readily available fuel for gasification testing. The energy content (EC) of the milo was determined by a Parr bomb calorimeter model 6200 (Parr Instrument Company, Moline, Ill.) and the moisture content by a Yamato model DX620 drying oven (Yamato Scientific America, Inc., Santa Clara, Cal.). The feed rate of the milo was calibrated with the motor speed driving the screw conveyor system. A Dart Controls model 253G-200E (Zionsville, Ind.) variable tachometer controlled the speed of the motor.

The energy loading (EL) and fuel to air (F/A) ratio were the two operational parameters for the gasifier. The EL is a function of the feeding rate and EC of the biomass per cross-sectional of the gasifier (eq. 10).

$$EL = \frac{\dot{m}_{fuel} \cdot EC \cdot 60}{A_{gasifier}} \quad (10)$$

where
EL = energy loading (GJ h^{-1} m^{-2})
$\dot{m}_{fuel}$ = feed rate of biomass fuel (kg min^{-1})
EC = energy content of biomass (GJ kg^{-1})
$A_{gasifier}$ = cross sectional area of gasifier (m^2).

The F/A ratio was used in part to determine the flow rate of ambient inlet air to the gasifier and was calculated by taking the ratio of the biomass to air feed rate, by mass. For cotton gin trash, a F/A ratio of approximately 0.2 kg_{fuel}/kg_{air} results in complete combustion (Maglinao et al., 2015). Capareda (2014) suggests that approximately 30% of the stoichiometric air requirement for combustion be used for gasification. This equates to a F/A ratio of approximately 0.5 kg_{fuel}/kg_{air}, which was the lower limit of F/A ratios when operating the gasifier.

A pre-analysis was performed prior to tests to determine if a proposed EL and F/A ratio would satisfy gasification operation. The EL determined the feed rate of the milo in the gasifier, which was then used to calculate the speed of the motor driving the screw conveyor. The air flow rate was determined from the F/A ratio and was verified to be within three air flow boundaries: MFV of the bed material, terminal velocity of the smallest bed particle, and terminal velocity of the biochar. The MFV and the terminal velocity of the biochar served as the lower bound air requirement, whereas the terminal velocity of the smallest bed particle was the upper bound. The temperature of the reaction was estimated to apply the appropriate density and viscosity of the air to the calculations. The terminal velocity of the biochar and smallest bed particle were calculated with the use of equations 11, 12, and 13 (Kunii and Levenspiel, 1991).

$$d_p{}^* = d_p\left[\frac{\rho_f \cdot (\rho_p - \rho_f) \cdot g}{\mu^2}\right]^{1/3} \tag{11}$$

$$V^* = \left[\frac{18}{(d_p{}^*)^2} + \frac{2.335 - (1.744 \cdot \Phi)}{(d_p{}^*)^{0.5}}\right]^{-1} \tag{12}$$

$$V_t = V^*\left[\frac{\mu \cdot (\rho_p - \rho_f) \cdot g}{\rho_f{}^2}\right]^{1/3} \tag{13}$$

where
d_p^* = dimensionless particle size
V^* = dimensionless gas velocity
V_t = terminal velocity (cm s^{-1}).

Gasification tests were divided into two stages: 1) locating an optimum combination of EL and F/A that achieved the highest quality of syngas, such that the operation was continuous and sustainable, and 2) operating a generator with syngas produced from the gasifier at the optimum operating parameters.

For the first stage, a starting combination of EL and F/A ratio was selected as 23.9 GJ h^{-1} m^{-2} and 1.0 kg_{fuel}/kg_{air}, respectively. It was hypothesized that this combination would result in the highest quality of syngas. Several tests were conducted by varying the EL and F/A ratio to determine the effect on the LHV of the syngas and temperature of the reaction. As the gasifier operated at the target combination of operational parameters, temperatures and pressures were observed to ensure the reaction was being carried out properly and safely. Tests were ran for a duration between one to two hours. For the duration, if the operation maintained a continuous and steady state reaction, then the test was deemed sustainable.

The optimum combination of EL and F/A ratio was used to operate the gasifier for generator testing. The syngas produced from the gasifier was directed to a 4kW Honda generator model GX240 (Alpharetta, Ga.) once the reaction reached steady state (the average temperature of the reaction remained relatively constant and did not fluctuate by more than ±10°C). Only a portion of the syngas produced was directed to the generator, while the excess was directed to the flare. Custom modifications to the engine of the generator were made so that the syngas could be the fuel for the engine. A

port was implemented in the duct of the engine between the air filter and the carburetor. The port connected the duct of the gasifier to the inlet of the engine, allowing the syngas to be mixed with the air for combustion in the engine.

Measurements taken during and after the gasification tests were used in several calculations to evaluate the process. The flow rate of the syngas at the venturi meter was used to calculate the conversion of fuel to syngas by mass and energy. When determining the energy conversion from fuel to syngas, the volumetric flow rate was converted to a standard flow rate and multiplied by the heating value, as seen in equations 14 and 15, respectively. The energy conversion efficiency was calculated by taking the ratio of the average energy in the syngas by the energy rate being loaded to the bed.

$$Q_{std} = Q_{act} \cdot \frac{\rho_{act}}{\rho_{std}} \tag{14}$$

where
Q_{std} = standard volumetric flow rate ($m^3\ min^{-1}$)
ρ_{act} = density of gas at actual conditions ($kg\ m^{-3}$)
ρ_{std} = density of gas at standard conditions ($kg\ m^{-3}$).

$$\eta_e = \frac{LHV_s \cdot Q_{std}}{EC \cdot \dot{m}_{fuel}} \cdot 100\% \tag{15}$$

where
η_e = energy conversion efficiency from fuel to syngas (%).

The conversion, by mass, of fuel to syngas (η_m) was approximated by equation 21. The mass flow rate of the inlet air was subtracted by that of the syngas, which determined the mass flow rate of gases from the fuel. The rate of gases generated by the fuel was divided by the input fuel feed rate to obtain the conversion of fuel to syngas.

$$\eta_m = \frac{\dot{m}_{syngas} - \dot{m}_{air}}{\dot{m}_{fuel}} \quad (16)$$

where
η_m = conversion of fuel to syngas by mass ($kg_{volatiles}/kg_{fuel}$)
$\dot{m}_{syngas}$ = mass flow rate of syngas (kg min^{-1})
$\dot{m}_{air}$ = mass flow rate of inlet air (kg min^{-1}).

The assumption was made that all of the biomass fuel was converted to either syngas or biochar. Therefore, the remaining percentage was assumed to be the conversion of fuel to biochar. After gasification tests, the mass of biochar captured was weighed. This weight was used to estimate the capture efficiency of the cyclone ($\eta_{cyclone}$) during operation by dividing the mass of the biochar captured by the estimated total biochar from the gasifier (eq. 17).

$$\eta_{cyclone} = \frac{m_{captured}}{m_{fuel} \cdot (1 - \eta_m)} \cdot 100\% \quad (17)$$

where
$\eta_{cyclone}$ = capture efficiency of cyclone (%)
$m_{captured}$ = mass of captured biochar (kg)
m_{fuel} = total mass of fuel used (kg)
T = total feeding time of fuel (min).

When calculating the capture efficiency of the tube cyclone during gasification, the biochar exiting the gasifier was assumed to not adhere to any of the surfaces within the system. The captured biochar was also analyzed by a Beckman Coulter Counter Multisizer 3 to determine the PSD.

One aspect to sizing the blower was estimating the total pressure drop throughout the system, which included the pressure drop through the cyclone. The TCD method was applied to calculate the cyclone's pressure drop constant, $K_{cyclone}$ (eq. 18). This constant

was used when calculating the pressure drop of the cyclone on the larger gasification system.

$$\Delta P_{cyclone} = K_{cyclone}(VP_{in} + VP_{out}) \quad (18)$$

where
$\Delta P_{cyclone}$ = cyclone pressure drop (kPa)
$K_{cyclone}$ = cyclone pressure drop constant (dimensionless)
VP = velocity pressure at inlet and outlet of the cyclone (kPa).

The velocity pressures at the inlet and outlet of the cyclone are a function of the gas velocities at those respective points (eq. 19).

$$VP = \frac{1}{2} \cdot v_{gas} \cdot \rho_{gas} \quad (19)$$

where
v_{gas} = velocity of gas (m s^{-1}).

The temperature was measured at the inlet of the cyclone to calculate the density of syngas at that point. Based on the mass flow rate of syngas measured by the venturi meter, the flow rate of the syngas can be calculated at the cyclone. Since the inlet and outlet dimensions of the cyclone were known, the velocities were calculated to determine the velocity pressures.

Fluctuations of the pressure gauges (± 0.5 kPa) were observed during the gasification process. Firstly, the compressor supplying air to the system operates in a pulsing manner, which causes the air flow rate to fluctuate. The feeding rate of the milo into the gasifier was not consistent. The combination of these two input fluctuations caused both the flow rate and the heating value of the syngas to have variation. To account for this variation, the average of all the data points of each measurement were taken for each test.

Results and Discussion

The moisture content (wet basis) and heating value of the milo were 12.6% and 16.36 MJ kg^{-1}, respectively. The moisture content of the milo was at a sufficient level such that no additional drying was needed before gasification. To ensure the moisture content would not increase, the milo was stored in a sealed barrel until the fuel was ready for gasification tests. The heating value of the milo was slightly higher than that of cotton gin trash, which is approximately 15.5 MJ kg^{-1} (LePori and Soltes, 1985).

The terminal velocity of the biochar and the smallest bed particle were 4.6 and 188 cm s^{-1}, respectively, at a temperature of 650°C (1200°F). The MFV was calculated to be 27 cm s^{-1} at these conditions. The diameters of the smallest bed particle, and biochar were 300 and 60 µm, respectively, while the mean bed particle diameter was 818 µm. The terminal velocity of the biochar was less than the MFV, thus making the MFV the lower bound air velocity. The difference between the MFV and the terminal velocity of the smallest bed particle (27 and 188 cm s^{-1}) allowed for a wide margin for the actual velocity when gasifying.

A preliminary gasification test was performed that had a target energy loading (EL) and fuel to air (F/A) ratio of 23.9 GJ h^{-1} m^{-2} and 1.0 kg_{fuel}/kg_{air}, respectively. For this test, the bed material was preheated to a temperature of 538°C before the milo was introduced at a feed rate of 0.45 kg min^{-1}. The temperature of the reaction had increased and peaked at approximately 632°C for a duration of around 20 minutes. Soon after this peak, the temperature steadily decreased to 600°C then suddenly dropped below 315°C, in which the operation was discontinued. The conclusion of the test was that the milo

was being over fed into the reactor. The feed rate of milo was greater than the rate of the reaction, causing the bed to cease fluidization. Once the temperatures of the gasifier had cooled to room temperature, visual inspection revealed a significant amount of residual milo that remained in the bed (fig. 15). Upon removing the bed material from the gasifier unit, a cluster of residual milo was observed at the screw conveyor.

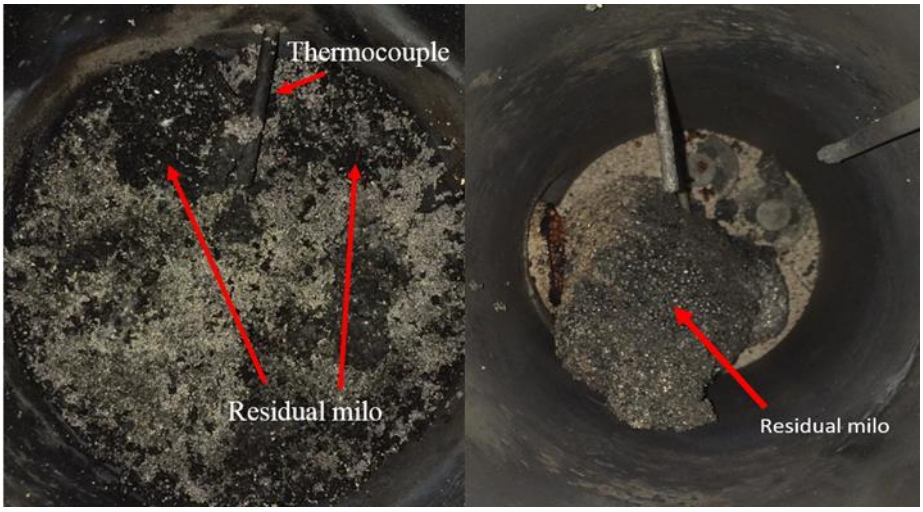

Figure 15. Significant amounts of residual milo in the bed (left) and at the screw conveyor (right) as a consequence of overloading the bed.

Although the preliminary gasification test was unsuccessful, knowledge was gained to properly operate the gasifier. A protocol was developed in which the fuel feed rate would be increased incrementally based on the temperature. Upon start up, the bed material would be preheated to 538°C. At this temperature, the propane burner would be turned off, the air flow rate set to the target rate, and the fuel introduced into the gasifier such that the F/A ratio is 0.5 kg_{fuel}/kg_{air}. Once the temperature reached 650°C, the F/A ratio would be increased to 0.6 kg_{fuel}/kg_{air}. At a temperature of 680°C, the F/A ratio

increased to 0.7 kg_{fuel}/kg_{air}. For any target F/A ratio greater than 0.7 kg_{fuel}/kg_{air}, the ratio would be increased incrementally by 0.1 kg_{fuel}/kg_{air} every 5 minutes. This would allow the operation to steadily approach the appropriate temperature of the reaction. During tests, the air flow rate was maintained constant and only the fuel feed rate was adjusted to vary the F/A ratio.

A total of 9 gasification tests were conducted in which the EL and F/A ratio were varied, shown in table 4. The response for these tests were the temperature of the reaction and lower heating value (LHV) of the syngas.

Table 4. Results of gasification tests by varying the EL and F/A ratio.

Test [#]	Energy Loading [GJ h^{-1} m^{-2}]	Fuel to Air Ratio [kg_{fuel}/kg_{air}]	Temperature of Reaction [°C]	Lower Heating Value of Syngas [MJ Nm^{-3}]
1	12.0	0.6	791	5.25
2	17.0	0.7	695	4.69
3	17.0	0.7	719	4.69
4	19.4	0.86	630	3.50
5	21.9	0.96	607	2.76
6	17.0	0.76	690	5.37
7	17.0	0.7	712	4.17
8	17.0	0.7	701	4.73
9	17.0	0.7	734	5.29

The temperature of the reaction was averaged between the upper and lower bed temperatures while the gasifier was operating under the target EL and F/A ratio. A general trend (fig. 16) was observed between F/A ratio and temperature of the reaction;

an increase in F/A ratio resulted in a decrease in the temperature. At a F/A ratio of 0.6 kg_{fuel}/kg_{air}, the temperature averaged at 791°C, while at a F/A ratio of 0.96 kg_{fuel}/kg_{air}, the temperature averaged at 607°C.

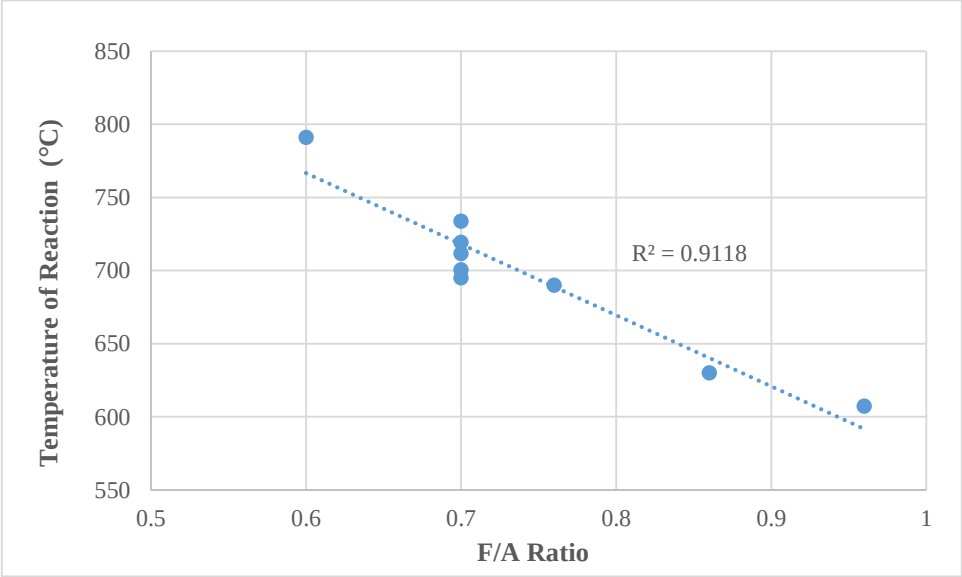

Figure 16. Decreasing trend of reaction temperature vs. increasing F/A ratio.

Gasification test 1 (table 4) was operated at a F/A ratio of 0.6 kg_{fuel}/kg_{air}, where the reaction temperatures reached up to 816°C. After approximately 90 minutes of operation for this test, the bed material became agglomerated (fig. 17). The ash of the milo had melted and adhered to the bed material particles, causing the bed to cease fluidization. Ceasing of fluidization of the bed material was realized by observing a sudden decrease in the temperature of the lower bed and increase in the upper bed. This indicated that the bed was no longer mixing for a near-isothermal region. At this point, gasification was discontinued. Therefore, it was concluded that the gasifier would be

operated at an upper limit reaction temperature of 732°C to ensure bed agglomeration did not occur. This correlated to operating the gasifier at a F/A ratio of 0.7 kg_{fuel}/kg_{air} and greater. However, reaction temperatures of up to 870°C have been used when gasifying cotton gin trash (LePori and Soltes, 1985).

Figure 17. Agglomerated bed material as a consequence of operating the gasifier at temperatures above the melting point of the ash.

The LHV of the syngas displayed a general trend (fig. 18) of decreasing by increasing the F/A ratio. LHVs of the syngas ranged between 5.25 and 2.76 MJ Nm^{-3} at F/A ratios of 0.6 and 0.96 kg_{fuel}/kg_{air}, respectively. The trend of the LHV of the syngas vs. F/A ratio appeared to be a consequence that the F/A had on the temperature. The water-gas shift and Boudouard reactions that produce the hydrogen and carbon monoxide combustible gases were favored at higher temperatures (Abdoulmoumine et al., 2014).

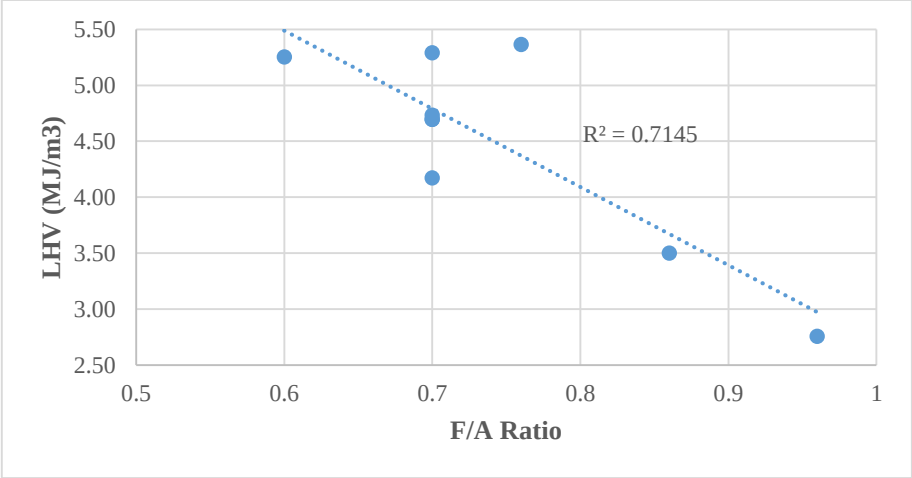

Figure 18. Decreasing trend of LHV vs. F/A ratio.

The volume fraction of the syngas components were relatively constant between each test conducted at an EL of 17.0 GJ h^{-1} m^{-2} and a F/A ratio of 0.7 kg_{fuel}/kg_{air}. Table 5 displays the gas chromatograph results from the gas sample of gasification test 3, which was calculated to have a heating value of 4.69 MJ Nm^{-3}. The primary contributors to the LHV of the syngas were the hydrogen, carbon monoxide, methane, and ethylene gas constituents. The gas chromatograph was calibrated only for the eleven gas components displayed in table 5. One compound that was not analyzed was steam. The summation of the volume percentages obtained from the gas analysis from all gasification tests ranged between 93% and 97%. The percentages of gas components were normalized to calculate the LHV of each syngas sample.

Table 5. Gas chromatograph results for gasification test 3.

Syngas Component	Volume (%)
Hydrogen	2.73
Oxygen	1.19
Nitrogen	56.77
Carbon Monoxide	16.06
Carbon Dioxide	12.50
Methane	2.32
Acetylene	0.20
Ethylene	1.57
Ethane	0.24
Propylene	0.02
Propane	0.01

The flow rate of the syngas calculated from the venturi meter was found to be inaccurate for gasification tests one through six. The mass flow rate of the syngas was calculated to be greater than the total input mass. This was a result of the biochar sticking to the surfaces of the constricted section of the venturi meter (fig. 19) as the gasifier was being operated. The accumulation of the biochar decreased the diameter of the constricted section. The change in the diameter affected the calculations for the flow rate of the syngas, thus resulting in inaccurate values.

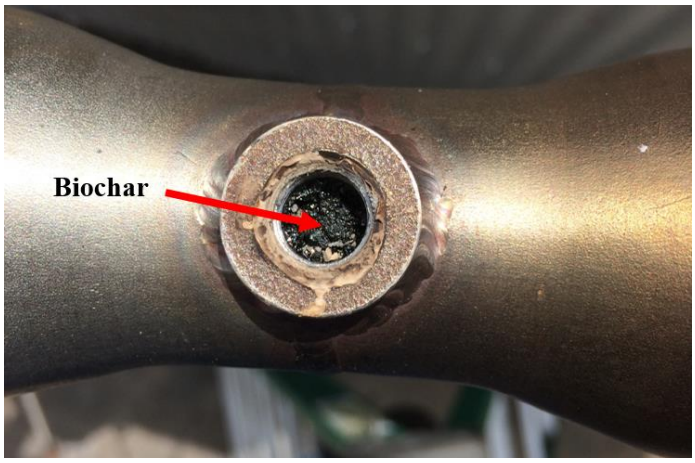

Figure 19. Accumulation of biochar observed through the pressure tap at the constricted section of the venturi meter.

To accurately measure the flow rate of the syngas, an outlet orifice meter was designed and manufactured from stainless steel. The estimated flow rate of the syngas leaving the cyclone was calculated to be 1 m^3 min^{-1} at an expected temperature of 316°C. The outlet orifice meter was designed based on the estimated flow rate such that the pressure drop across the orifice would accurately measure the flow while not causing excessive back pressure in the system.

The outlet orifice meter replaced the venturi meter and was used for gasification test seven (table 6). The average flow rate of the syngas was 0.96 m^3 min^{-1} at an average temperature of approximately 343°C. This equates to an average mass flow rate of 0.56 kg min^{-1}, shown in table 6. The minimum and maximum recorded mass flow rates were 0.51 and 0.60 kg min^{-1}, respectively.

Table 6. Results of operating the gasifier at an EL of 17.0 GJ h^{-1} m^{-2} and a F/A ratio of 0.7 kg_{fuel}/kg_{air}.

Parameter	Minimum	Maximum	Average	Std. Deviation
Mass flow of syngas (kg min^{-1})	0.51	0.60	0.56	0.02
Mass conversion of fuel to syngas (%)	22	54	39	0.07
Energy conversion of fuel to syngas[a] (%)	34	40	38	0.02

a. LHV of syngas was 4.17 MJ Nm^{-3}

For each recorded data point in test seven, the conversion of fuel to syngas was calculated based on the mass flow rates of inlet air, fuel, and syngas. Mass conversions of fuel to syngas ranged from 22% to 54% with an average of 39%.

At a fuel feed rate of 0.32 kg min^{-1}, the energy being loaded to the bed was 5.17 MJ min^{-1}. The average energy rate of the syngas ranged between 1.78 and 2.1 MJ min^{-1}, with an average of 1.96 MJ min^{-1}. This equated to energy conversions ranging between 34% and 40% with an average of 38%.

One gas sample was extracted during gasification test seven which had a LHV of 4.17 MJ Nm^{-3}. This LHV was assumed to be constant when calculating the minimum and maximum values of energy conversion for the gasification test (table 5). The LHV at the operating conditions for test seven were expected to be greater, ranging between 4.47 and 5.22 MJ Nm^{-3}. Therefore, the energy conversions of fuel to syngas reported were conservative.

The estimated capture efficiency of the tube cyclone for test seven was inconclusive. It was observed that a significant amount of biochar adhered to surfaces of

the cyclone (fig. 20). An alternative approach and additional research is needed to more accurately predict the capture efficiency of the tube cyclone while operating the gasifier.

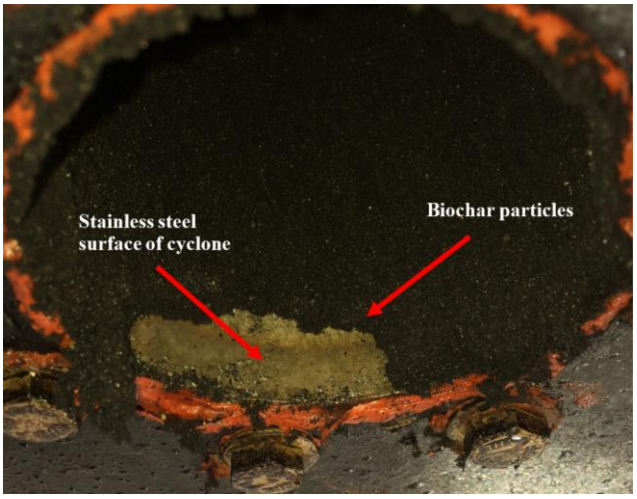

Figure 20. Biochar particles adhering to the inner surface of the cyclone.

The particle density of the biochar captured from test seven was found to be 0.9 g cm^{-3}. The PSD of the biochar captured by the tube cyclone had a best fit MMD of 16 µm (AED) and a GSD of 1.9 (fig. 21). The best fit MMD and GSD was determined by taking the average theoretical MMD and GSD from each of the three biochar samples. The characteristics of the biochar particulate exhibit that of a lognormal function based on the mass fraction at a given particle diameter.

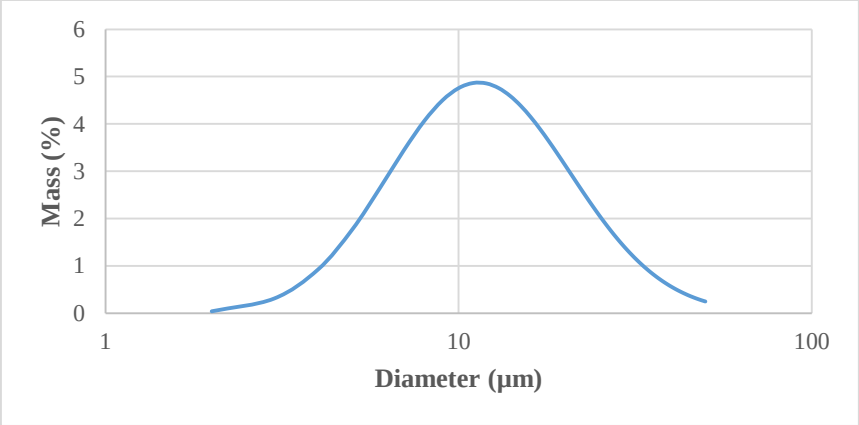

Figure 21. PSD of captured biochar with an average MMD of 16 µm (AED) and GSD of 1.9.

The tube cyclone's pressure drop constant ($K_{cyclone}$) had an average value of 5.7 during test 7, as shown in table 7. The minimum and maximum calculated $K_{cyclone}$ values were 4.9 and 7.2, respectively.

Table 7. Characteristics of tube cyclone during gasification test 7.

Parameter	Minimum	Maximum	Average	Std. Deviation
$\Delta P_{cyclone}$ (kPa)	1.2	1.42	1.3	0.05
$K_{cyclone}$	4.9	7.2	5.7	0.52
Temperature (°C)	361	441	414	22.4
Flow rate (m^3 min^{-1})	1	1.19	1.1	0.05

For gasification tests eight and nine, the generator was connected to the gasification system. The outlet orifice meter was moved to the bottom of the T-section (fig. 22) so that the flow rate of the syngas to the engine could be measured. The venturi

meter was placed in the system to connect the cyclone to the T-section; no measurements were taken from the venturi meter for the two tests.

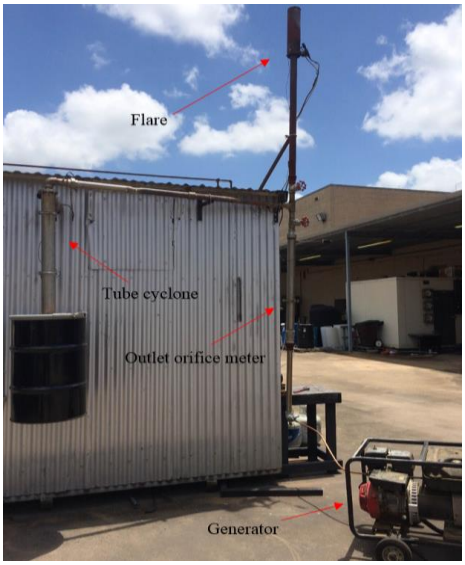

Figure 22. Generator test set up for gasification.

Once steady state gasification was achieved at an EL of 17.0 GJ h^{-1} m^{-2} and a F/A ratio of 0.7 kg_{fuel}/kg_{air}, the 4 kW generator was started and fueled by gasoline. The point when the engine started to struggle after the gasoline valve was closed, the syngas was introduced to the generator through the engine's carburetor. For both gasification tests, the engine was successfully and continuously fueled solely by syngas. The duration that the engine was fueled by syngas without human intervention ranged between 15 and 20 minutes before being manually shut down.

The temperatures of the hot syngas going to the generator were approximately 370°C in which a portion of tars were condensing. Tars are higher hydrocarbons that

condense at relatively high temperatures. During generator operation, the temperature of the hot syngas sustained the condensed tars as a liquid. At the completion of generator tests, however, once the engine had cooled, the observation was made that tars had solidified within the system, including the inlet of the combustion chamber. The solidified tars prevented the inlet valve from opening and closing while attempting to start the engine. The tars were cleaned from the inlet valve in order to operate the engine for future tests. In order to prevent the tars from solidifying and clogging the inlet of the engine, a method to properly clean out the liquid tars needs to be incorporated in the shutdown procedure to prevent damage to the engine.

Summary and Conclusions

A preliminary fluidized bed gasification (FBG) test was conducted at an energy loading (EL) of 23.98 GJ h^{-1} m^{-2} and a fuel to air (F/A) ratio of 1.0 kg_{fuel}/kg_{air}. The feed rate of the milo was found to be greater than the rate that the milo was being gasified, resulting in an overloading of the bed. From this test, a new protocol was developed to properly operate the gasifier.

A total of nine gasification tests were conducted in which the EL and F/A ratio were varied to determine the effect on the operating temperature and the lower heating value (LHV) of the syngas. General trends were observed in which an increase in the F/A ratio resulted in a decrease in the operating temperature and a decrease in the LHV of the syngas.

At an optimum combination of EL of 17.0 GJ h^{-1} m^{-2} and a F/A ratio of 0.7 kg_{fuel}/kg_{air}, the average LHV of the syngas was approximately 4.72 MJ Nm^{-3} at an average reaction temperature of 700°C. This combination of EL and F/A ratio was selected to achieve the highest LHV of the syngas while ensuring the process be continuous.

The venturi meter measuring the flow rate of the syngas at the outlet of the cyclone was reporting incorrect values. Biochar particles penetrating the cyclone were adhering to the surfaces of the constricted section of the venturi meter, which was changing the diameter of the section which was affecting flow rate calculations.

A stainless steel outlet orifice meter was designed that replaced the venturi meter. The outlet orifice meter was used to calculate the flow rate and temperature of the syngas. The average mass flow rate of the syngas was 0.56 kg min^{-1} at an EL of 17.0 GJ h^{-1} m^{-2} and a F/A ratio of 0.7 kg_{fuel}/kg_{air}. The conversion of fuel to gas by mass and energy were 39% and 38%, respectively.

The estimated capture efficiency of the biochar from the tube cyclone during gasification was inconclusive. This was due to a portion of the biochar particles adhering to the cyclone's surface.

A 4 kW generator was successfully fueled solely by syngas during gasification. A portion of the syngas from the system was directed to the generator, in which the generator was being operated continuously for up to 20 minutes. Once the generator was running continuously, the entire system was self-sustaining, not requiring any human intervention.

Tars were observed to condense to the inlet of the combustion chamber of the engine. Once the engine had cooled, the tars had solidified which caused the inlet valve to the combustion chamber to remain stationary while the engine was attempted to be started. An engine that is designed to for dirty gas operations should replace the gasoline engine since the gasoline engine was not designed for the syngas from the gasifier.

CHAPTER V

SUMMARY AND CONCLUSIONS

Three important aspects were investigated in this study to properly and sustainably operate a pilot scale fluidized bed gasification (FBG) system for electricity generation: 1) minimum fluidization velocity of the bed material, 2) tube cyclone performance for biochar capture, and 3) determining the optimum operating parameters of the pilot scale FBG system that results in a sustainable production of syngas for electricity generation. Based on the data obtained from the pilot scale system, a FBG system that generates 500 kW of electricity can be designed.

The first aspect that was investigated was the minimum fluidization velocity (MFV) of the bed material. Tests were conducted at ambient conditions in a Plexiglass chamber designed similar to the fluidized bed reactor. The bed material used in the ambient tests was also used during gasification tests. A total of nine tests were conducted to evaluate the average experimental at ambient conditions. The theoretical MFV was calculated by using equation 2. The average experimental and theoretical MFV at ambient conditions was 56.0 and 63.5 cm s^{-1}, respectively. The experimental and theoretical MFVs were within reason to conclude that equation 2 provided an accurate estimate of the MFV of the bed material. From this, it was concluded that equation 2 would accurately predict the MFV of the bed material at the operating conditions of gasification.

A byproduct of FBG is biochar, an ash-like particulate conveyed out of the reactor with the syngas. Before combustion of the syngas in an internal combustion engine (ICE), the biochar concentration needs to be reduced to prevent slagging and fouling. A stainless steel tube cyclone was designed and evaluated for biochar capture. A vortex inverter was thought to be placed at the natural length of the cyclone during operation for maximum capture efficiency. Ambient air tests were conducted that varied both the air flow rate and the vortex inverter position. Capture efficiencies ranged between 95% and 99%. Both the flow rate (between 1 and 1.4 m^3 min^{-1}) and vortex inverter position (between 4D and 10D) had an insignificant effect on the capture efficiency of the tube cyclone. Since the vortex inverter position did not affect the capture efficiency, additional cyclone tests were conducted in which the vortex inverter was removed. The tube cyclone achieved between 96% and 98% capture efficiencies without the vortex inverter in the cyclone. The conclusions from the ambient tube cyclone tests was that the capture efficiency could be expected to be above 95% during gasification, and that the vortex inverter was not needed.

Gasification tests were separated into two stages: 1) determining an optimum combination of energy loading (EL) and fuel-to-air (F/A) ratio of the gasifier that results in a sustainable production of the highest achievable quality of syngas and 2) validating the concept of electricity generation by directing the syngas to a generator at the optimum combination of EL and F/A ratio. The biomass fuel used in this study was grain sorghum (milo) since it can be uniformly fed in the pilot scale gasifier. Milo also

has a similar energy content to that of cotton gin trash (CGT), which is approximately 16.3 MJ kg^{-1}.

The optimum combination of EL and F/A ratio was determined to be 17.0 GJ h^{-1} m^{-2} and 0.7 kg_{fuel}/kg_{air}, respectively. At this combination, the average lower heating (LHV) of the syngas was 4.72 MJ Nm^{-3}, while the energy conversion of fuel to syngas was approximately 38%. An EL at 23.9 GJ h^{-1} m^{-2} resulted in overloading the reactor, causing an accumulation of biomass that ultimately ceased fluidization of the bed. The highest achieved LHV of the syngas was 5.25 MJ Nm^{-3} at a F/A ratio of 0.6 kg_{fuel}/kg_{air}. However, the reaction temperature (816°C) at this F/A ratio was above the melting point of the ash, resulting in an unsustainable process by causing the bed material to become agglomerated. Increasing the F/A ratio to 0.7 kg_{fuel}/kg_{air} decreased the reaction temperature to approximately 700°C in which the process was sustainable.

Additional research is needed to accurately predict the capture efficiency of the tube cyclone during gasification. The capture efficiency was estimated by determining the ratio of the captured biochar to the estimated total input. During gasification tests, biochar particles were adhering to the surfaces of the cyclone, affecting the mass of captured biochar.

The syngas produced by operating the pilot scale FBG system at the optimum operating parameters was directed to a 4 kW Honda generator. The generator was fueled solely by the syngas produced from the pilot scale system, which validated electricity generation from syngas. Human intervention was not required while both the FBG system and the generator were being operated, displaying a sustainable process for

electricity generation. Assuming a generator efficiency of 35% and an energy conversion from fuel to syngas of 38%, an overall efficiency is calculated to be approximately 13%. Prior to this research, an overall efficiency of 10% was expected.

Overall, a significant advancement has been made towards the implementation of a FBG system to provide cotton gins with a means of generating their own electricity. Although the electricity demand for a cotton gin is on the order of MWs, a 500 kW FBG system serves as a stepping stone to achieve that demand. The results from this research demonstrated that FBG is an alternative, reliable method for electricity production at a cotton gin.

Future Research and Work

The conclusions drawn from the gasification of milo will serve as guidelines as the project progresses. The next step of the project will be to adjust the current pilot scale FBG system to gasify (CGT). Currently, the feed rate of CGT is too low to operate the gasifier at the optimum combination of EL and F/A ratio. Additional gasification tests will need to be conducted to determine the combination of EL and F/A ratio that result in the highest achievable LHV of the syngas, while ensuring the process is continuous and self-sustaining.

The conversions of CGT to syngas by energy and mass at the optimum combination of EL and F/A will first need to be determined on the pilot scale FBG system. Once the necessary data has been collected, the FBG system that generates 500 kW can be designed. The energy conversion efficiency and the EL will be used to size

the gasifier unit, while the conversion of CGT to syngas by mass and the F/A ratio will be used to size the cyclone to capture biochar.

An alternative approach to predict the capture efficiency of the tube cyclone during gasification needs to be developed. This involves determining a method that accurately measure the total amount of biochar that is being conveyed to the cyclone. A method to prevent the biochar from adhering to the surfaces of the cyclone also needs to be determined.

Sustaining the temperatures of the syngas downstream of the gasifier should be investigated to minimize the amount of tars condensing. Maintaining the tars in vapor form as the syngas is combusted in the internal combustion engine is hypothesized to increase the overall heating value of the syngas as compared to the tars condensing. In addition, an engine designed for dirty gas operations should be investigated as it is better suited for being fueled by syngas.

REFERENCES

Abdoulmoumine, N., A. Kulkarni, and S. Adhikari. 2014. Effects of Temperature and Equivalence Ratio on Pine Syngas Primary Gases and Contaminants in a Bench-Scale Fluidized Bed Gasifier. *Industrial& Engineering Chemistry Research*. *53: 5767-5777*.

Capareda, S.C. 1990. Studies on Activated Carbon Produced from Thermal Gasification of Biomass Wastes. PhD diss. College Station, Texas: Texas A&M University, Department of Agricultural Engineering.

Capareda, S. C. 2014. *Introduction to Biomass Energy Conversions*. Sound Parkway, NW. Taylor and Francis Group.

Cooper, C. D. and F. C. Alley. 2011. *Air Pollution Control.* 4th ed. Long Grove, Illinois. Waveland Press, Inc.

Hoffmann, A. C., R. de Jonge, H. Arends and C. Hanrats.1995. Evidence of the 'Natural Vortex Length' and its Effect on the Separation Efficiency of Gas Cyclones. Filtration & Separation 32.8 (1995): 799-804.

Kunii, D., and O. Levenspiel. 1991. *Fluidization Engineering. Second Edition*. Newton, Massachusetts. Butterworth-Heinemann.

LePori, W. A., R. G. Anthony, R. B. Griffin, T. C. Pollock, A. R. McFarland, and C. B. Parnell, Jr. (1981). *Biomass energy conversion using fluidized-bed technology: Beyond the energy crisis, 4*:A297 – A304. New York: Pergamon Press.

LePori, W.A, and C. B. Parnell, Jr. 1983. *Clean-up of gases produced from gasification of agricultural biomass*. College Station, Texas: Texas A&M University, Department of Agricultural Engineering.

LePori, W.A. and E. J. Soltes. 1985. *Biomass Energy; A Monograph*. College Station, Texas. Texas A&M University Press.

LePori, W. A. and R. Egg. 1994. Residue Use as Fuel. In *Managing Agricultural Residues,* 343-376. Boca Raton, Florida. CRC Press, Inc.

Luehrs, D.R. 2014. Reducing PM Concentrations in Simulated High Temperature Gas Streams. MS thesis. College Station, Texas: Texas A&M University, Department of Biological and Agricultural Engineering.

Maglinao, A. L. 2013. Development of a Segregated Municipal Solid Waste Gasification System for Electrical Power Generation. PhD diss. College Station, Texas: Texas A&M University, Department of Biological and Agricultural Engineering.

Maglinao, A. L., S. C. Capareda, and H. Nam. 2015. Fluidized bed gasification of high tonnage sorghum, cotton gin trash and beef cattle manure: Evaluation of synthesis gas production. *Energy Conversion and Management 105: 578 – 587.*

Olofsson, G., Z. Ye, I. Bjerle, and A. Andersson. 2002. Bed Agglomeration Problems in Fluidized-Bed Biomass Combustion. *Ind. Eng. Chem. Res. 41(12):* 2888-2894.

Rhodes, M. 2008. *Introduction to Particle Technology*. 2nd ed. West Sussex, England. John Wiley & Sons Ltd.

Saucier, D. S. 2013. Cyclone Performance for Separation of Biochar from Syngas Produced by Gasification of Cotton Gin Trash. Thesis. College Station, Texas: Texas A&M University, Department of Biological and Agricultural Engineering.

TCGA. 2006. TCGA Gin Operating Cost Survey 2006. Texas Cotton Ginners Association, Austin, Texas.

USDA. 2015. Cotton Production in Texas: 2014. National Agricultural Statistics Database. Washington, D.C.: USDA National Agricultural Statistics Service. Available at: www.nass.usda.gov. Accessed 2 July 2015.

APPENDIX

Appendix A. Sample PSD Analysis of Bed Material

Test:		**3**			
Total Mass, g		**417.3**			
Diameter Range (µm)		**Midpoint, dp**	**Mass In Range**	**Fraction in Range, x**	**x/dp**
Lower	**Upper**	**[µm]**	**[g]**		
1000	-	1000	158.7	0.380	4E-04
500	1000	750	253.8	0.608	8E-04
355	500	427.5	3.6	0.009	2E-05
297	355	326	0.6	0.001	4E-06
250	297	273.5	0.6	0.001	5E-06
-	250	250	0	0	0
				SUM	0.001
				Mean Particle Size (µm)	**819**

The midpoint between the test sieves was used as the average particle size when using equation 7. The upper (1000 µm) and lower (250 µm) test sieves were used as the midpoint size for particles captured on the top sieve and capture bucket, respectively.

Appendix B. Screw Conveyor Calibration

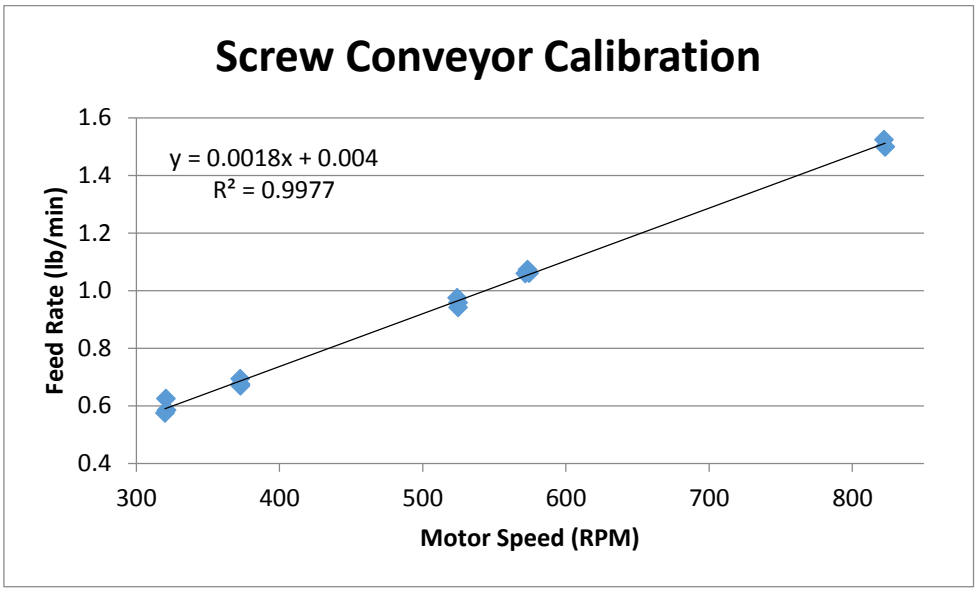

Motor [RPM]	Feed Rate [lb/min]
573	1.1
572	1.1
574	1.1
524	1.0
525	0.9
525	1.0
373	0.7
372	0.7
373	0.7
320	0.6
321	0.6
321	0.6
822	1.5
823	1.5
823	1.5

Appendix C. Sample Calculations for Gasification Performance

Energy efficiency from fuel to syngas:

Data from gasification:

Milo feed rate = 0.7 lb/min at 7000 Btu/min.

Flow rate of syngas = 34 actual ft^3/min at 0.036 lb/ft^3.

LHV of syngas = 125 Btu/std.ft^3.

Equations 19 and 20;

$$Q_{std.} = \frac{\left(34\,\frac{ft^3}{min}\right)*(0.036\frac{lb}{ft^3})}{0.075\,(\frac{lb}{ft^3})} = \textbf{16 std.ft}^{\textbf{3}}\textbf{/min}$$

$$\eta_e = \frac{(16\,\frac{std.ft^3}{min})*(125\frac{Btu}{std.ft^3})}{\left(0.7\frac{lb}{min}\right)*(7000\frac{Btu}{lb})} * 100\% = \textbf{40\%}$$

Conversion of fuel to syngas by mass:

Data from gasification:

Milo feed rate = 0.7 lb/min.

Air flow rate = 1 lb/min.

Flow rate of syngas = 36 actual ft^3/min at 0.035 lb/ft^3 = 1.26 lb/min.

Equation 21;

$$\eta_m = \frac{\left(1.26\,\frac{lb_{syngas}}{min}\right)-(1\,\frac{lb_{air}}{min})}{0.7\,\frac{lb_{milo}}{min}} *100\% = \textbf{38\%}$$

Appendix D. Sample Calculations for 500 kW Gasifier

Cotton Gin Trash Feed Rate:

Efficiency from fuel to syngas = 38%

Efficiency from syngas to electricity = 35%

Energy Content = 7000 $\frac{Btu}{lb}$

Output = $500\ kW * \frac{3412\frac{Btu}{hr}}{kW}$ = 1.71 $\frac{MMBtu}{hr}$

Overall Efficiency = 38%*35% = 13.3%

Input = $\frac{Output}{Efficiency} = \frac{1.71\ \frac{MMBtu}{hr}}{13.3\%}$ = 12.8 $\frac{MMBtu}{hr}$

Input = (Feed Rate)*(Energy Content)

Feed Rate = $\frac{12.8\ x\ 10^6\ \frac{Btu}{hr}}{7000\ \frac{Btu}{lb}}$ = **1830** $\boldsymbol{\frac{lb}{hr}}$

Reactor Diameter:

EL = 1.5 $\frac{MMBtu}{hr-ft^2}$

Area = $\frac{(Feed\ Rate)*(Energy\ Content)}{EL} = \frac{\left(1830\ \frac{lb}{hr}\right)*(7000\frac{Btu}{lb})}{1.5\ x\ 10^6\frac{Btu}{hr-ft^2}}$ = 8.54 ft^2

Diameter = $\sqrt{\frac{4}{\pi} * A} = \sqrt{\frac{4}{\pi} * 8.54 ft^2}$ = **3.3 ft**

Appendix E. Technical Specifications of GX240 Honda Engine

GX240/GX270 (PTO shaft type S)

Length × Width × Height		355 × 430 × 410 mm (14.0 × 16.9 × 16.1 in)
Dry mass [weight]		25.0 kg (55.1 lbs)
Engine type		4-stroke, overhead valve, single cylinder
Displacement [Bore × Stroke]	GX240	242 cm³ (14.8 cu-in) [73.0 × 58.0 mm (2.9 × 2.3 in)]
	GX270	270 cm³ (16.5 cu-in) [77.0 × 58.0 mm (3.0 × 2.3 in)]
Net power (in accordance with SAE J1349*)	GX240	5.3 kW (7.2 PS, 7.1 bhp) at 3,600 rpm
	GX270	6.0 kW (8.2 PS, 8.0 bhp) at 3,600 rpm
Max. Net torque (in accordance with SAE J1349*)	GX240	15.3 N·m (1.56 kgf·m, 11.3 lbf·ft) at 2,500 rpm
	GX270	17.7 N·m (1.80 kgf·m, 13.1 lbf·ft) at 2,500 rpm
Engine oil capacity		1.1 ℓ (1.2 US qt , 1.0 Imp qt)
Fuel tank capacity		5.3 ℓ (1.40 US gal , 1.17 Imp gal)
Cooling system		Forced air
Ignition system		Transistor magneto
PTO shaft rotation		Counterclockwise